Article

Supramolecular Photochirogenesis Driven by Higher-Order Complexation. Enantiodifferentiating Photocyclodimerization of 2-Anthracenecarboxylate to Slipped Cyclodimers via 2:2 Complex with #-Cyclodextrin

Xueqin Wei, Wanhua Wu, Ryohei Matsushita, Zhiqiang Yan, Dayang Zhou, Jason J. Chruma, Masaki Nishijima, Gaku Fukuhara, Tadashi Mori, Yoshihisa Inoue, and Cheng Yang

J. Am. Chem. Soc., **Just Accepted Manuscript** • DOI: 10.1021/jacs.7b12085 • Publication Date (Web): 13 Feb 2018

Supramolecular Photochirogenesis Driven by Higher-Order Complexation. Enantiodifferentiating Photocyclodimerization of 2-Anthracenecarboxylate to Slipped Cyclodimers via 2:2 Complex with β-Cyclodextrin

Xueqin Wei,[†,#] Wanhua Wu,[†,#] Ryohei Matsushita,[‡,#] Zhiqiang Yan,[†,#] Dayang Zhou,[§] Jason J. Chruma,[†,⊥] Masaki Nishijima,[¶] Gaku Fukuhara,[∥] Tadashi Mori,[‡] Yoshihisa Inoue,*[,‡] and Cheng Yang*[,†]

[†] *Key Laboratory of Green Chemistry & Technology, College of Chemistry, State Key Laboratory of Biotherapy, West China Medical Center, Healthy Food Evaluation Research Center, and* [⊥] *Sino-British Materials Research Institute, College of Physical Sciences and Technology, Sichuan University, 29 Wangjiang Road, Chengdu, 610064, China*

[‡] *Department of Applied Chemistry and* [¶] *Office for University-Industry Co-creation, Osaka University, Yamada-oka, Suita565-0871, Japan*

[§] *Comprehensive Analysis Center, ISIR, Osaka University, Mihogaoka, Ibaraki 567-0047, Japan*

[∥] *Department of Chemistry, Tokyo Institute of Technology, 2-12-1 Ookayama, Meguro-ku, Tokyo 152-8551, Japan*

Emails: inoue@chem.eng.osaka-u.ac.jp; yangchengyc@scu.edu.cn

[#] *Equal contributions.*

ABSTRACT: Chiral slipped 5,8:9',10'-cyclodimers were preferentially produced over classical 9,10:9',10'-cyclodimers upon supramolecular photocyclodimerization of 2-anthracenecarboxylate (AC) mediated by β-cyclodextrin (β-CD). This photochirogenic route to the slipped cyclodimers, exclusively *head-to-tail* (HT) and highly enantioselective, has long been overlooked in foregoing studies but is dominant in reality and is absolutely supramolecularly activated by 2:2 complexation of AC with β-CD. The intricate structural and photophysical aspects of this higher-order complexation-triggered process were comprehensively elucidated, while the absolute configurations of the slipped cyclodimers were unambiguously assigned by comparing the experimental versus theoretical circular dichroism spectra. In the 2:2 complex, two ACs packed in a dual β-CD capsule are not fully overlapped with each other but only partially stacked in slipped *anti*- or *syn*-HT manner, and hence do not spontaneously cyclodimerize upon photoexcitation but emits long-lived excimer fluorescence at wavelengths slightly longer than the monomer fluorescence, indicating that the slipped excimer is neither extremely reactive nor completely relaxed in conformation and energy. Due to the slipped conformation of the AC pair in soft capsule, the subsequent photocyclodimerization becomes manipulable by various internal/external factors, such as temperature, pressure, added salt, and host modification, enabling us to exclusively obtain the slipped cyclodimers in high regio- and enantioselectivities. In this supramolecularly driven photochirogenesis, the dual β-CD capsule functions as a chiral organophotocatalyst to trigger and accelerate the nonclassical photochirogenic route to slipped cyclodimers by pre-organizing the conformation of encapsulated AC pair, formally mimicking catalytic antibody.

INTRODUCTION

Manipulating physical property and chemical reactivity of organic molecule through noncovalent interaction is one of the most crucial goals in current photochemistry and supramolecular chemistry.[1,2] By forming supramolecular assembly, guest molecule(s) are spatially confined, orientationally aligned, conformationally restricted, and locally concentrated in a limited space of host cavity to alter the original properties and reactivities. Indeed, (chiral) molecular hosts, such as cyclodextrin,[3] cavitand,[4] cucurbituril,[5] coordination cage,[6] and hydrogen-bonding template,[7] have been employed for controlling excited-state properties and reactivities through supramolecular assembling[8] to achieve substantial changes in chiroptical property and stereochemical outcome in chirality sensing[9] and photochirogenesis.[1-8]

Anthracenes have long been a target of intensive photochemical research, which makes the photocyclodimerization of anthracenes one of the most established and utilized photoreactions.[10] Upon photoexcitation, anthracenes usually undergo the orbital symmetry-allowed [4+4] cyclodimerization at 9,10-positions, whereas [6+6], [4+2], and [2+2] cyclodimerization, as well as slipped [4+4] cyclodimerization at 1,4- or 5,8-positions, rarely occur.[10b,c] These unconventional photocyclodimerization routes are occasionally triggered by the electronic and/or steric effects of substituent(s) introduced to anthracene,[11] but have never been activated by supramolecular complexation.

A pioneering work on the supramolecular [4+4] photocyclodimerization of 1-, 2-, and 9-anthracenecarboxylate and 1- and 2-anthracenesulfonate mediated by β- and γ-cyclodextrin (CD) was reported by Tamaki et al. in mid-1980s.[12] They found that γ-CD greatly accelerates the photocyclodimerization of 2-anthracenecarboxylate and 1- and 2-anthracenesulfonate as a result

of the simultaneous inclusion of two anthracene guests in a γ-CD cavity. Of particular interest, they reported that β-CD also accelerates the photocyclodimerization of 2-anthracenecarboxylate and -sulfonate to preferentially afford *anti-head-to-tail*(*anti*-HT)-9,10:9',10'-cyclodimer, without mentioning about the formation of any irregular cyclodimers.[12b,c]

In our further attempts to reinvestigate the photocyclodimerization of 2-anthracene-carboxylate (AC) mediated by β-CD[12] from the photochirogenic viewpoint,[13,14] we revealed that β-CD not merely shifts the product selectivity to *anti*-HT-9,10:9',10'-cyclodimer **1** but unexpectedly activates the nonclassical reaction pathway to slipped *anti*- and *syn*-HT-5,8:9',10'-cyclodimers **5** and **6** (Scheme 1). In this work, we first elucidate the chemical structures and absolute configurations of these new chiral 5,8:9',10'-cyclodimers, as well as the complexation and photocyclodimerization mechanisms. Then, we will demonstrate that the present supramolecular photochirogenic system, involving 2:2 complex, is highly susceptive to and hence readily manipulable by various environmental factors and host modification to achieve the exclusive formation of the slipped cyclodimers in high enantioselectivities. Finally, we will discuss the origin and significance of this unique supramolecular photochirogenic reaction driven by higher-order complexation in a wider perspective of organocatalysis and catalytic antibody.

Scheme 1. Supramolecular 1:1 and 2:2 Complexation of 2-Anthracenecarboxylate (AC) with Native β-Cyclodextrin (β-CD) and its Cationic Derivatives (**7**-**12**) and Subsequent Photocyclodimerization to Classical 9,10:9',10'-Cyclodimers **1**-**4** and Nonclassical 5,8:9',10'-Cyclodimers **5** and **6**

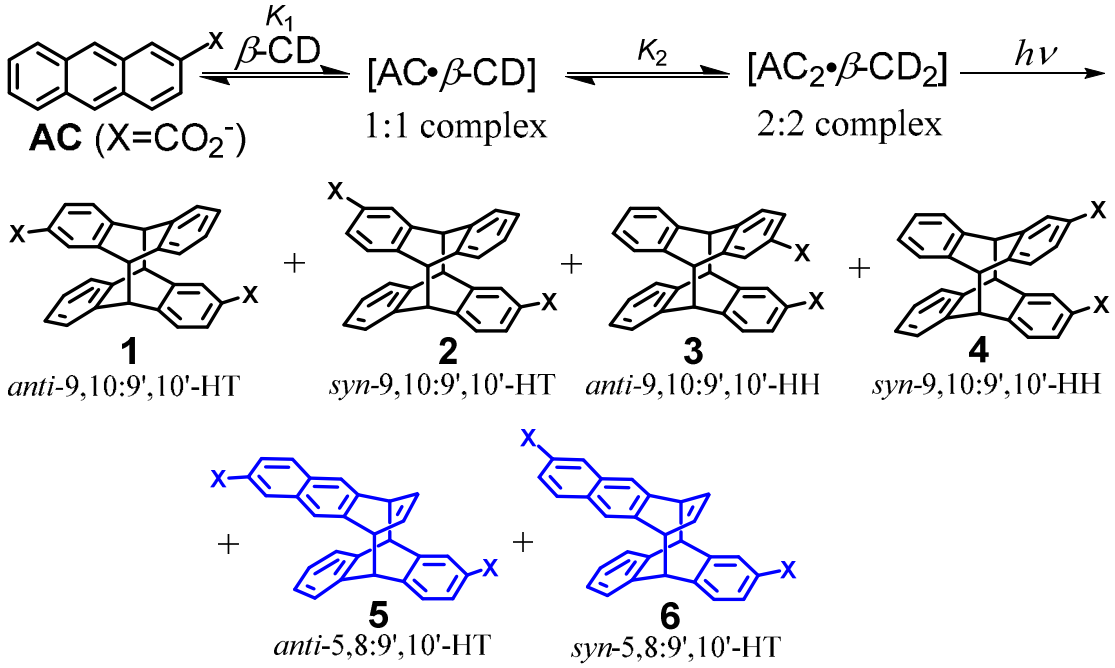

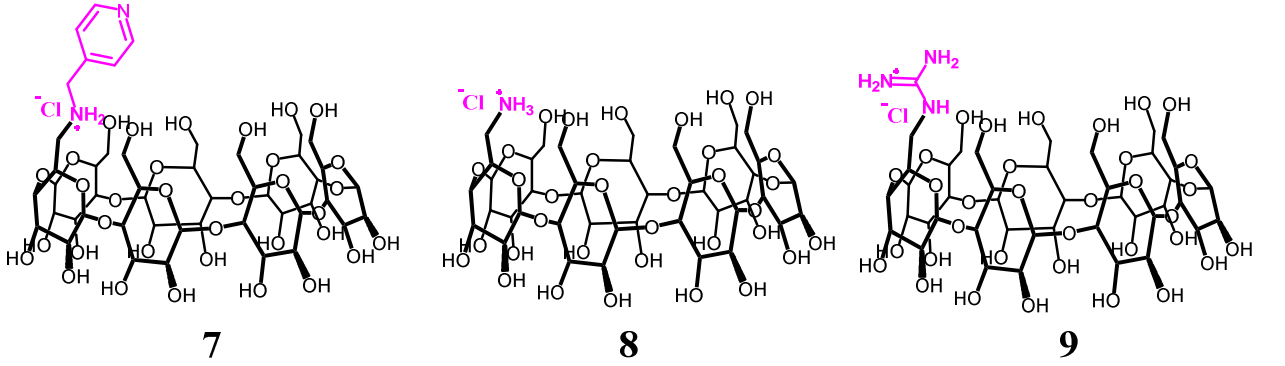

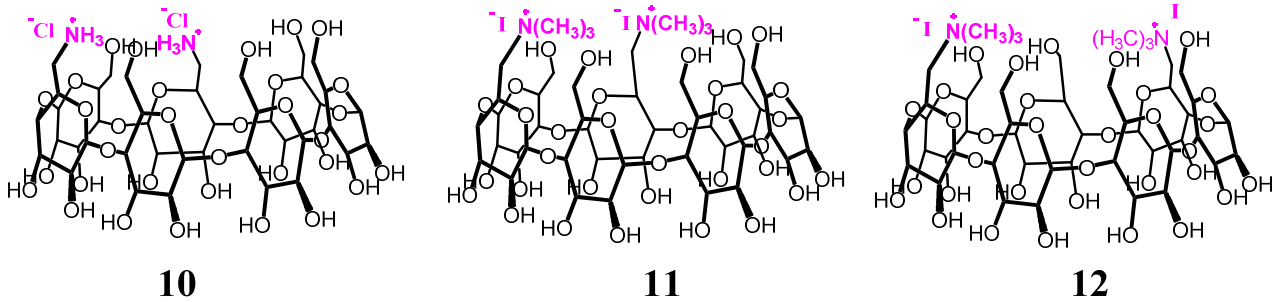

RESULTS AND DISCUSSION

Slipped 5,8:9',10'-Cyclodimers 5 and 6. Photoirradiation of AC (0.2 mM) with *β*-CD (4 mM) was performed in phosphate buffer solution (PBS) at pH 9. The irradiated sample was subjected to chiral HPLC analysis[13a] to reveal the formation of unidentified photoproducts in addition to conventional cyclodimers **1-4**. Under the HPLC conditions employed, these new products started to elute immediately after cyclodimer **4** and spread over a wide range of retention time; see Figure S1[15] for the chiral HPLC traces monitored by serial circular dichroism and fluorescence detectors. Crucially, the circular dichroism monitoring showed that the four new peaks are assignable to the enantiomer pairs of two chiral products, while the fluorescence monitoring at 420 nm with excitation at 340 nm (where **1-4** are transparent and hence fluorometrically silent) implied that these new products carry a naphthalene chromophore. HPLC analysis of the sample on achiral ODS column showed two major peaks (Figure S2),[15] which were collected separately to provide pure **5** (4.5% yield) and **6** (3.0% yield) (Figure S3;[15] see also Figure S4[15] for the separation of enantiomers). Cyclodimer **6** was totally stable at least for 12 days in the eluent stored at room temperature in the dark, showing no appreciable changes upon HPLC examinations before and after the storage; sharing the same skeleton, cyclodimer **5** is expected to behave similarly.

MS spectra of **5** and **6** showed the molecular ion peaks at *m/z* 443 (Figures S5 and S6),[15] indicating that they are also AC dimers isomeric to **1-4**. ^{1}H and ^{13}C NMR spectra of **5** and **6** closely resemble to each other (Figure 1; also compare Figure S9 with S10 and Figure S13 with S14).[15] In the ^{1}H NMR spectra (Figures 1 and S7-S10),[15] 14 aromatic and 4 nonaromatic proton signals were observed for both **5** and **6**, while two nonequivalent carboxylic and 24 aromatic carbons in the ^{13}C NMR spectra (Figures S11-S15),[15] revealing the unsymmetrical nature of **5**

and **6**. In addition, the four aromatic proton singlets observed indicate that the central aromatic ring of one AC moiety is preserved in the cyclodimers.

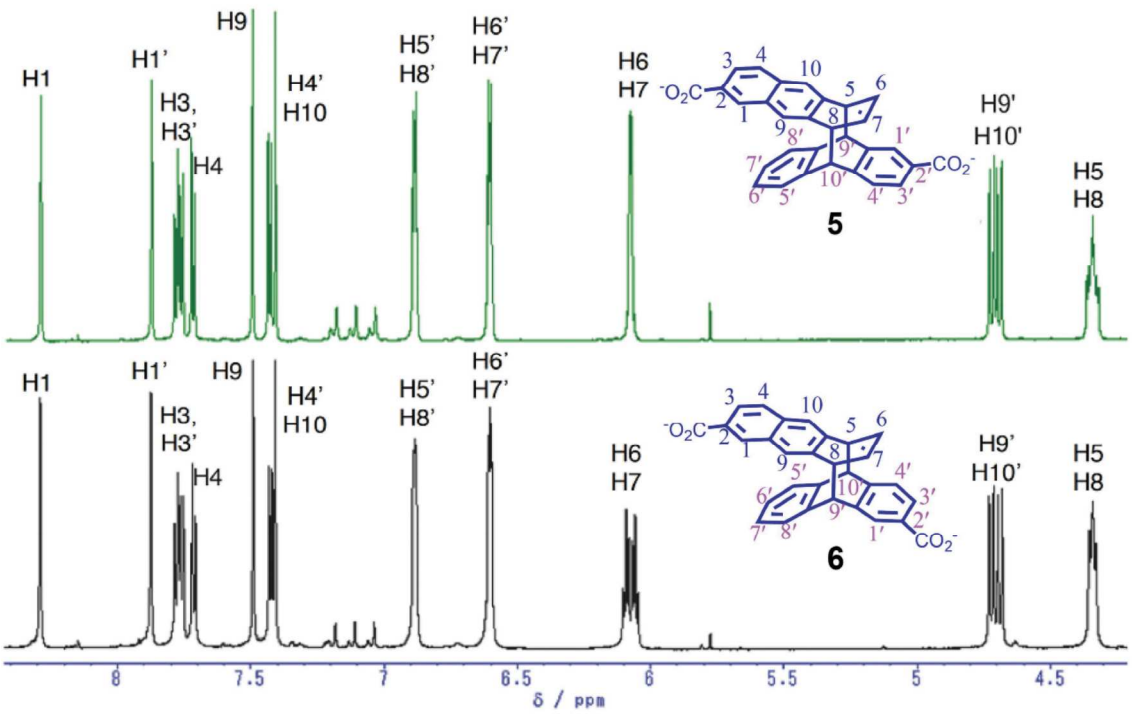

Figure 1. ^{1}H NMR spectra of **5** and **6** in DMSO-d_6 at 25 °C.

To elucidate the structures of **5** and **6**, several 2D NMR techniques were employed (Figures S16-S37).[15] Thus, the HSQC spectra were obtained to assign the protonated carbon resonances, while the coupling network of neighboring protons was elucidated by ^{1}H-^{1}H COSY. By combining the results obtained by long-range proton-carbon correlation ^{1}H-^{13}C HMBC and NOESY, the quaternary carbons and the relative positions of all carbons and protons were unequivocally assigned, allowing us to determine the structures of **5** and **6** as *anti*- and *syn*-HT-5,8:9',10'-cyclodimers (Scheme 1), respectively.

The structural similarity of **5** and **6** led to the nearly superimposable UV-vis spectra over the entire range (Figure 2, solid lines). In comparison to classical cyclodimers **1** and **3**, slipped **5** and **6**, possessing a naphthalene chromophore, absorb at much longer wavelengths; the 0-0 transition of the lowest-energy ^1L_b band is bathochromically shifted by 9.2 nm relative to that of unsubstituted 2-naphthoate (Figure 2, dashed line). On the other hand, the UV-vis spectra of **5** and **6** in the high-energy region are not a simple summation or average of those of 9,10:9',10'-cyclodimer and 2-naphthoate, suggesting strong electronic interactions between the facing naphthalene and benzene chromophores.

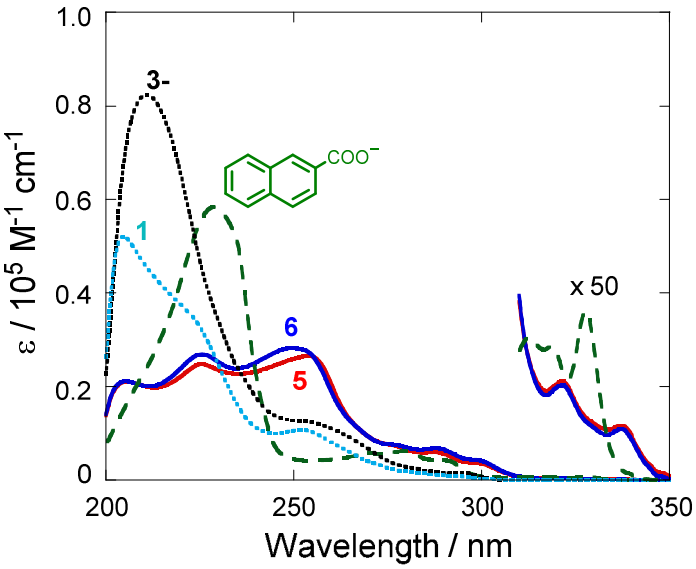

Figure 2. UV-vis spectra of cyclodimers **1** (cyan), **3** (black), **5** (red) and **6** (blue) and reference 2-naphthoate (green) in alkaline methanol (NaOH) at 25 °C.

Chiroptical Properties and Absolute Configurations of Enantiomeric 5,8:9',10'-Cyclodimers 5 and 6. Slipped cyclodimers **5** and **6** were resolved by preparative chiral HPLC to give optically pure enantiomer pairs of $\mathbf{5}_+/\mathbf{5}_-$ and $\mathbf{6}_+/\mathbf{6}_-$ (Figure S4),[15] where the subscripts +/- are tentative tags to identify the first/second fractions eluted from the chiral column employed (OJ-

RH). As shown in Figure 3, *anti*- and *syn*-isomeric **5** and **6** gave analogous UV-vis but distinctly different circular dichroism spectra. The enantiomer pairs exhibited mirror-imaged circular dichroism spectra with relatively large anisotropy factors ($g = \Delta\varepsilon/\varepsilon$) of 2-4 x 10^{-3} at the main band, presumably due to the rigid skeleton that fixes the transition moments of neighboring chromophores at defined angles.

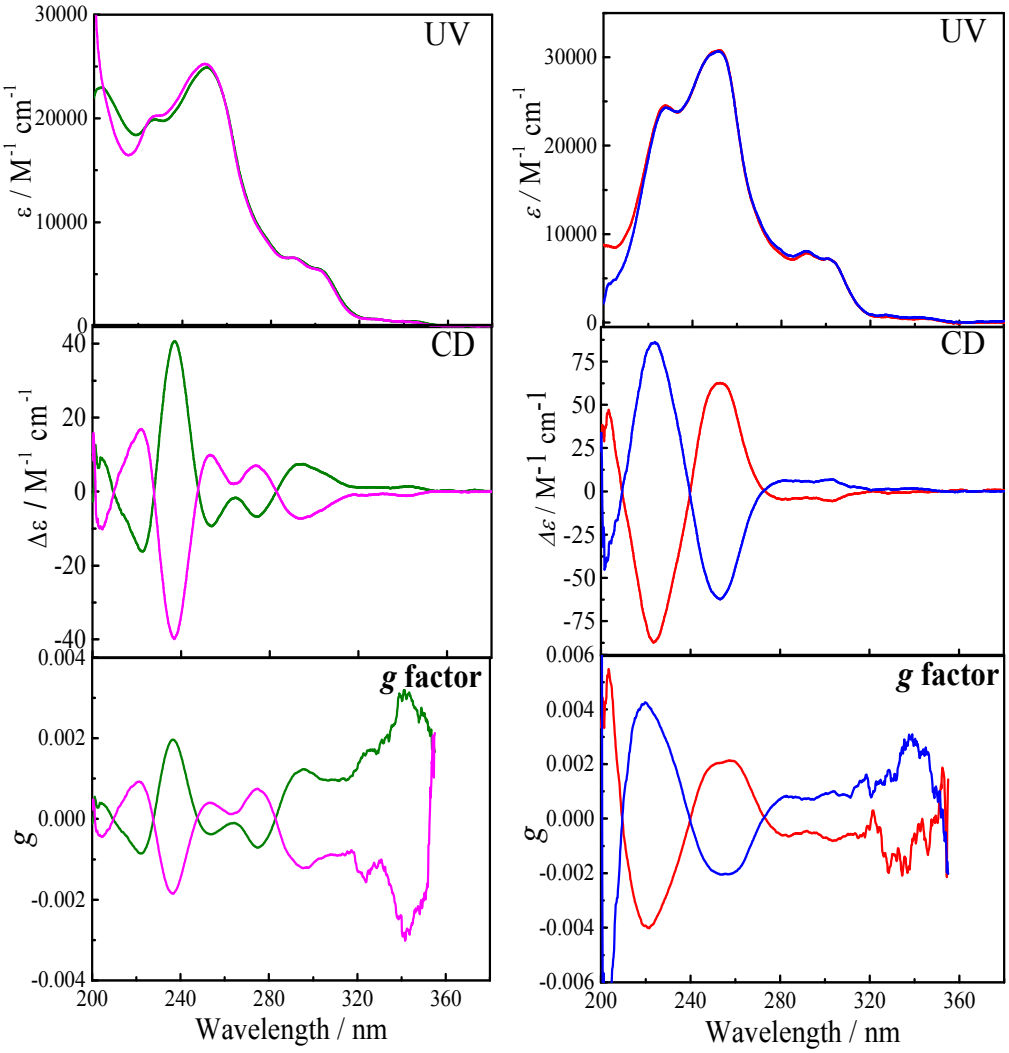

Figure 3. UV-vis (top), circular dichroism (middle), and anisotropy (*g*) factor (bottom) spectra of enantiopure $\mathbf{5}_+$ (10.2 μM) (green), **5-** (8.3 μM) (magenta), $\mathbf{6}_+$ (3.8 μM) (red), and **6-** (3.5 μM) (blue) in PBS (pH 9.0) at 25 °C.

The absolute configurations of **5**$_+$/**5**$_-$ and **6**$_+$/**6**$_-$ were determined by comparing the experimental circular dichroism spectra with the theoretical simulations at the RI-CC2/def2-TZVPP level.[16] As can be seen from Figure 4, the experimental circular dichroism spectrum of **5**$_+$ is in good agreement with the theoretical spectrum calculated for (5*S*,8*R*:9'*S*,10'*R*)-**5**, and the experimental spectrum of **6**$_+$ agrees with the theoretical one calculated for (5*S*,8*R*:9'*S*,10'*R*)-**6**; for the optimized geometries, see Tables S1 and S2.[15]

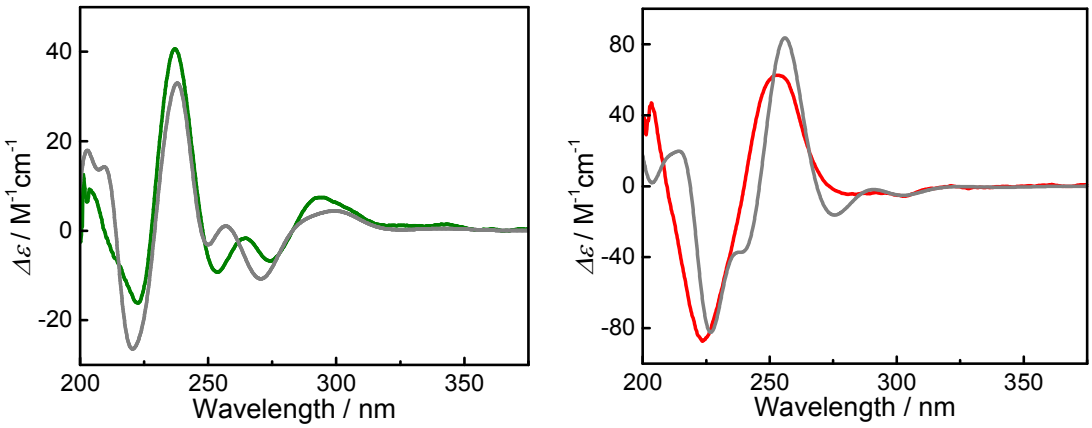

Figure 4. Experimental CD spectra of first-eluted **5**$_+$ (green) and **6**$_+$ (red) measured in PBS, on which overlaid are the theoretical spectra calculated for (5*S*,8*R*:9'*S*,10'*R*)-**5** and (5*S*,8*R*:9'*S*,10'*R*)-**6** at the RI-CC2/TZVPP level (red-shifted by 0.3 eV) (gray), respectively.

Higher-Order Complexation of AC with *β*-CD. Variable temperature ^{1}H NMR spectra of AC (2 mM) were recorded in the presence of *β*-CD (4 mM) in a D_2O solution at pD 9.0 (Figures 5 and S38).[15] As shown in Figure 5, by lowering the temperature from 50 to 5 °C, AC's H5-H8 protons located farthest from the carboxylate greatly shifted to the upfield by 0.47-1.21 ppm with accompanying peak broadening, while H9 and H10 exhibited much smaller upfield shifts of 0.07-0.17 ppm and the H1, H3, and H4 near the carboxylate showed no practical shifts. Thus, the

degree of upfield shift decreased in the order: H6 > H7 > H5 > H8 >> H9 > H10 >> H4 > H3 and H1, indicating partial overlap of the two included AC molecules at the far edge (from the carboxylate). This trend significantly differs from that observed for the 2:1 complexation of AC with γ-CD,[13a] where all of the aromatic protons experience large upfield shifts due to the full stacking of two AC molecules in the cavity. The magnitudes of chemical shift changes observed upon VT-NMR nicely correlate with the population of 2:2 complex that increases with deceasing temperature (Figure 5, right column).

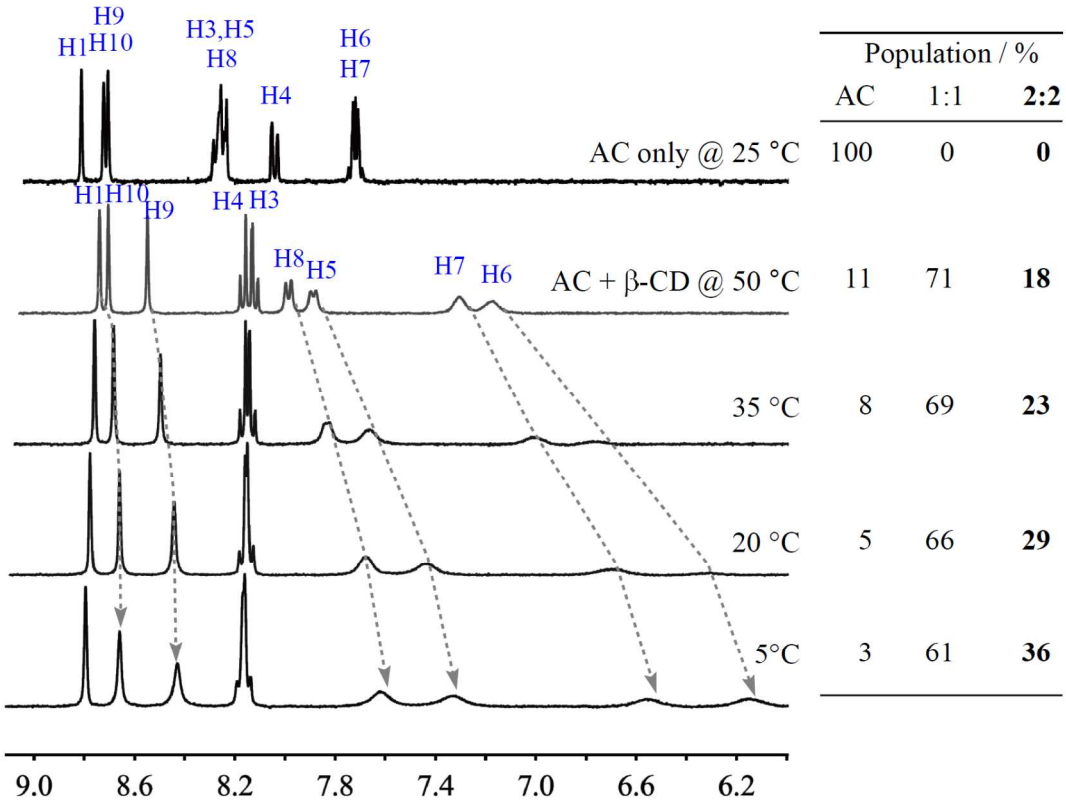

	Population / %		
	AC	1:1	**2:2**
AC only @ 25 °C	100	0	**0**
AC + β-CD @ 50 °C	11	71	**18**
35 °C	8	69	**23**
20 °C	5	66	**29**
5°C	3	61	**36**

Figure 5. VT ^{1}H NMR spectra of AC (2 mM) with β-CD (4 mM) in a phosphate-buffered D_2O solution (pD 9.0) at 50, 35, 20, and 5 °C; the molar population of free AC, 1:1, and 2:2 complex at each temperature was calculated by using the thermodynamic parameters shown in Table 1 (vide infra).

The orientation of included AC in β-CD cavity was elucidated by using the ROESY technique. As shown in Figure 6, the H5' proton on the interior wall near the primary rim of β-CD gave crosspeaks with AC's H1, H3, and H4, as well as H9 and H10, while H3' located near the secondary rim of β-CD only correlated with H8 (weak), H9, and H10. Crucially, no clear crosspeaks were observed between H5-H7 of AC and H3' or H5' of β-CD, partially due to the peak broadening. These ROESY results unequivocally indicate that the carboxylate-bearing benzene ring of AC is oriented toward the primary rim and positioned in between H3' and H5' of β-CD, while the central ring is located near the secondary rim, leaving the terminal ring outside the cavity (Figure 6, inset). Combining the ROESY results with the above-mentioned stronger shielding effects observed particularly for H5-H8 on the terminal ring at lower temperatures, we conclude that the 2:2 complex is formed through the association of two 1:1 complexes from the secondary rim, where the terminal aromatic ring of AC is somewhat exposed to facilitate further assembly to the 2:2 complex through π-π stacking. It is likely therefore that the formation of 1:2 or 2:1 complex is not feasible, and free AC and 1:1 and 2:2 complexes become the major species in the solution. As can be seen from the VT-NMR spectra (Figure 5), the 2:2 complex is a minor species at higher temperatures but rapidly grows in population by lowering the solution temperature.

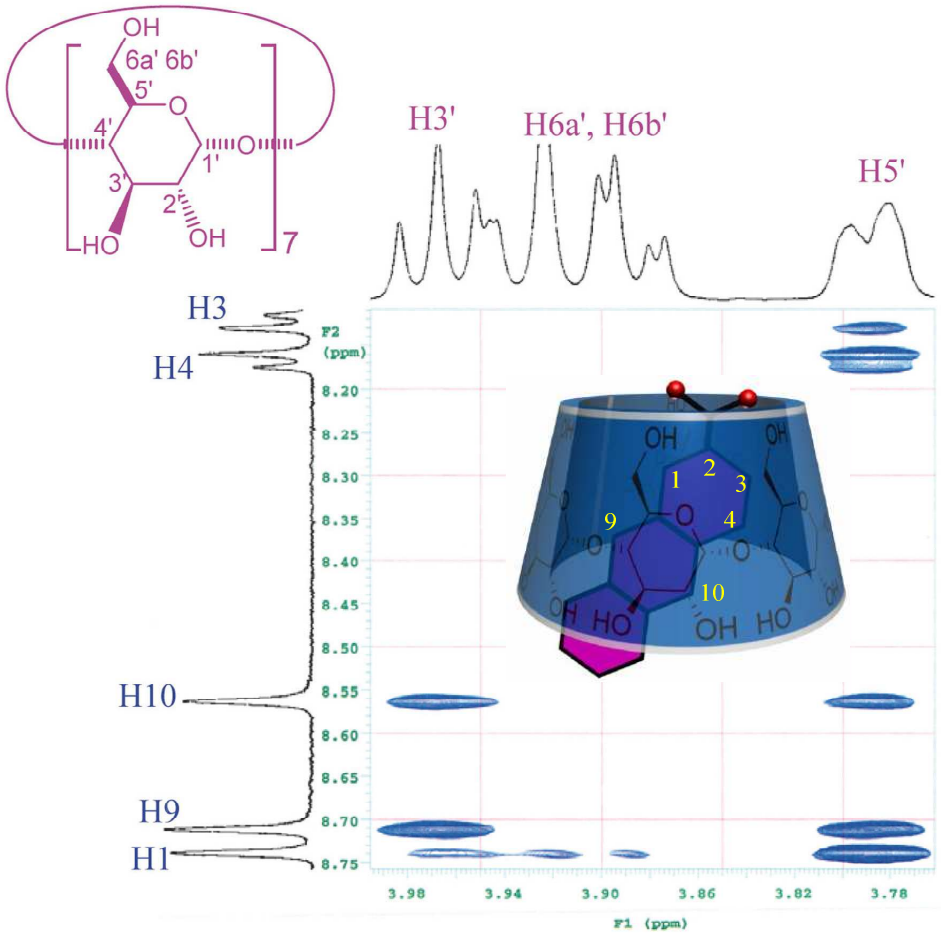

Figure 6. Partial ROESY spectrum of a phosphate-buffered D_2O solution (pD 9.0) of AC (2 mM) and β-CD (4 mM) at 25 °C and the estimated position of AC in the CD cavity (inset). Under the conditions employed, the population of free AC, 1:1 complex, and 2:2 complex is 8:66:26, and hence the crosspeaks are considered to arise from both the complexes.

For better illustrating the stacking geometry of 2:2 complex, we performed the molecular modeling study using the dispersion-corrected DFT method at the DFT-D3(BJ)-TPSS/def2-SV(P) level[18] to obtain the structures simulated for the *re-re, si-si,* and *re-si* complexes. As can be seen from Figure S39,[15] two AC molecules are stacked to each other but sled by one to one-and-a-half benzene units, which is in good agreement with the position of AC in the β-CD cavity

estimated from the NMR ROESY study (Figure 6). It is also to note that the two β-CDs are held together by a hydrogen-bonding network interweaving the facing β-CD's secondary rims.

To quantitatively evaluate the complexation of AC with β-CD, we performed the UV-vis and circular dichroism spectral titrations in PBS at 25 °C. As shown in Figure 7a, addition of β-CD to a solution of AC (0.2 mM) induced small bathochromic shifts of the ^1B_b and ^1L_a bands of AC with accompanying isosbestic points, suggesting less extensive stacking interaction. This issue will be discussed later in relation to the excimer fluorescence.

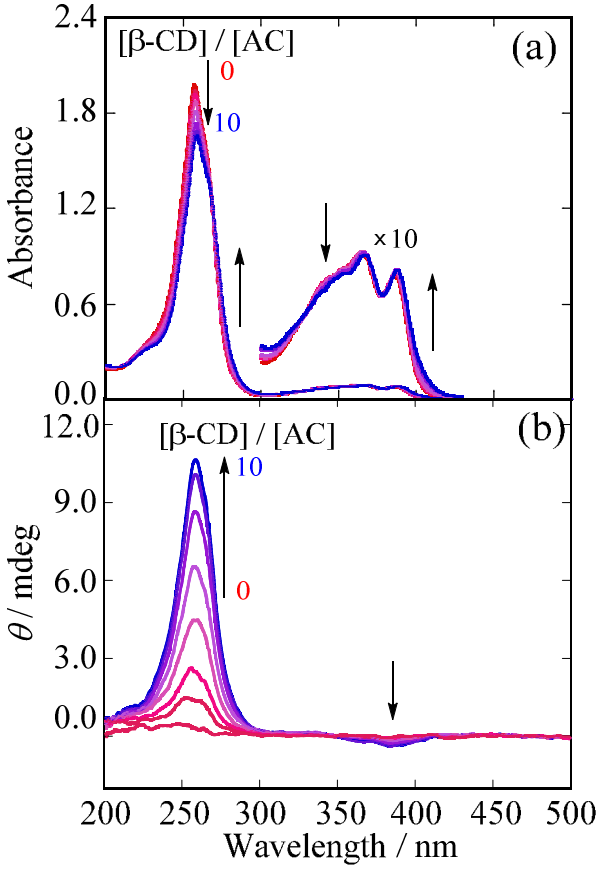

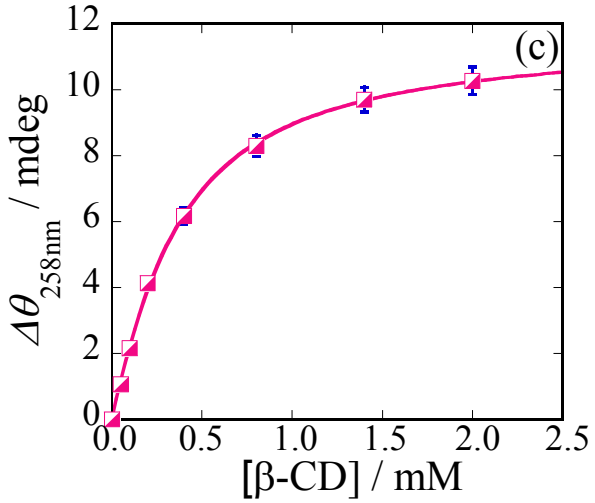

Figure 7. (a) UV-vis and (b) circular dichroism spectral changes of AC (0.2 mM) upon titration with *β*-CD (0-2 mM) in PBS (pH 9.0) at 25 °C; measured in a 1 mm cell. (c) Nonlinear least squares fit of the ellipticity changes ($\Delta\theta$) at 258 nm, assuming the stepwise 1:1 and 2:2 complexation.

In the circular dichroism spectral titration (Figure 7b), gradual addition of *β*-CD induced a positive Cotton effect at the ^1B_b band and a negative one at the ^1L_a band. According to the empirical "sector rule" proposed by Kajtár et al.,[19] these induced Cotton effect signs indicate that AC longitudinally penetrates into the CD cavity as illustrated in Figure 6, where the longitudinal ^1B_b and transversal ^1L_a transitions are respectively aligned parallel and orthogonal to the CD axis. The UV-vis spectral Job plots obtained at 0.5 °C for the solutions of AC and *β*-CD at a fixed total concentration of 0.2 mM (Figures S40-S42)[15] reached the maximum at molar fraction 0.5, indicating formally *n*:*n* but practically 1:1 stoichiometry. The lack of a bisignate exciton couplet in the circular dichroism spectrum (Figure 7b) did not appear to support the contribution of 2:2 complex at least at this low total concentration (0.2 mM). Nevertheless, the circular dichroism spectral titration data (Figure 7b) did not fit to the simple 1:1 complexation model (Figure S43)[15]

but were reasonably analyzed by assuming stepwise 1:1 and 2:2 complexation (equations 1 and 2), as shown in Figure 7c, to give a relatively large 1:1 association constant (K_1) of 3800 M^{-1} and a much smaller 2:2 association constant (K_2) of 150 M^{-1}. In this relation, Hamai[20a] and Bohne[20b,c] have reported that β-CD similarly forms 1:1 and 2:2 complexes with naphthalene derivatives, but the K_2 values are much larger than the corresponding K_1 values, leading to highly efficient 2:2 complexation. Crucially, β-CD and 2-anthracenesulfonate form 1:1 and 2:2 complexes with the K_1 value larger than K_2,[20a] as is exactly the case with the present system (Table 1). This and our present results indicate that the anthracene moiety provides strong hydrophobic interaction with β-CD favorable for the 1:1 complexation but the steric bulk makes the 2:2 complexation less favorable.

$$K_1 = [\mathrm{AC}\bullet\beta\text{-CD}]/[\mathrm{AC}][\beta\text{-CD}] \quad (1)$$

$$K_2 = [\mathrm{AC}_2\bullet\beta\text{-CD}_2]/[\mathrm{AC}\bullet\beta\text{-CD}]^2 \quad (2)$$

By using the K_1 and K_2 values obtained, the population of free AC, 1:1, and 2:2 complex was calculated to be 12:84:4 for an aqueous solution containing 0.2 mM AC and 2.0 mM β-CD at 25 °C. This low molar population (4%) of the 2:2 complex even at the highest host concentration employed in the titration experiment (Figure 7) may rationalize the apparent lack of exciton couplet in the circular dichroism spectra. Similar titration experiments at 0.5 and 50 °C (Figure S44)[15] and the subsequent fitting of the titration data to equations 1 and 2 (Figure S45)[15] gave the K_1 and K_2 values at these temperatures, as listed in Table 1.

Table 1. Thermodynamic Parameters for the 1:1 and 2:2 Complexation of AC with β-CD in PBS at pH 9.0

stoichio-	tempera-	CsCl/M	K/M^{-1}	$\Delta G°$/	$\Delta H°$/	$T\Delta S°$ [a]/

metry	ture/°C			kJ mol^{-1}	kJ mol^{-1}	kJ mol^{-1}
1:1	50	0	1900 ± 30			
	25	0	3800 ± 50	-20.4 ± 0.1	-22.6 ± 0.1	-2.2 ± 0.1
		0.5	4400 ± 30			
		6.0	5500 ± 90			
	0.5	0	8500 ± 100			
2:2	50	0	90 ± 10			
	25	0	150 ± 30	-12.4 ± 0.5	-16.5± 0.1	-4.1 ± 0.1
		0.5	230 ± 10			
		6.0	300 ± 30			
	0.5	0	270 ± 30			

[a] T = 298 K.

The K_1 value of 3800 M^{-1} obtained for AC at 25 °C is reasonable as an association constant with β-CD, when compared with those for benzoate (K_1 = 16 M^{-1}) and 2-naphthoate (K_1 = 320 M^{-1}).[21] The much smaller K_2 value of 150 M^{-1}, although no corresponding values have been reported for the lower homologues, is also sensible if the limited extra space remaining in the 1:1 complex and the partial π-overlap at the far-edge of AC are taken into consideration. For a better thermodynamic understanding of the 1:1 and in particular the 2:2 complexation, the association constants at different temperatures (Table 1) were subjected to the van't Hoff analyses to give straight lines for both the stoichiometries (Figure S46),[15] from the slope and intercept of which the enthalpy ($\Delta H°$) and entropy ($\Delta S°$) changes upon 1:1 and 2:2 complexation were calculated as listed in Table 1. The thermodynamic parameters thus obtained indicate that both the 1:1 and 2:2 complexation are obviously enthalpy-driven with much smaller entropic losses. The significantly smaller free energy of complexation for the 2:2 complexation ($\Delta\Delta G° = \Delta G°_{1:1} - \Delta G°_{2:2}$ = -8.0 kJ mol^{-1}) is traced back mainly to the smaller enthalpic gain ($\Delta\Delta H°$ = -6.1 kJ mol^{-1}) and somewhat to the larger entropic loss ($T\Delta\Delta S°$ = 1.9 kJ mol^{-1}), the former of which would be attributable to the less extensive hydrophobic and π-stacking interactions and the latter to the repositioning of

AC guest in the CD cavity upon assembling two 1:1 complexes. These thermodynamic parameters also allow us to calculate the population of free and complexed AC species at any concentration and temperature. Thus, the significant NMR upfield shifts of H5-H8 protons in AC (Figure 5) are reasonably accounted for in terms of the population of the 2:2 complex enhanced to 36% in a solution containing 2 mM AC and 4 mM β-CD at 5 °C.

Fluorescence Spectral Studies. The excited-state properties of AC–β-CD complexes were first examined by fluorescence spectroscopy. In the absence of β-CD, AC (2 μM) emitted broad fluorescence at 426 nm in PBS (Figure 8a, red) without showing any sign of excimer fluorescence at longer wavelengths. However, when β-CD (5 mM) was added to this solution, the AC fluorescence was appreciably reduced in intensity and exhibited vibrational fine structures (Figure 8a, blue), indicating inclusion of AC in the hydrophobic CD cavity. Under the conditions employed, the population of 2:2 complex was calculated as negligible 0.05% (while those of free AC and 1:1 complex were 5.00% and 94.95%, respectively), and hence the spectroscopic changes were reasonably attributed to the 1:1 complexation.

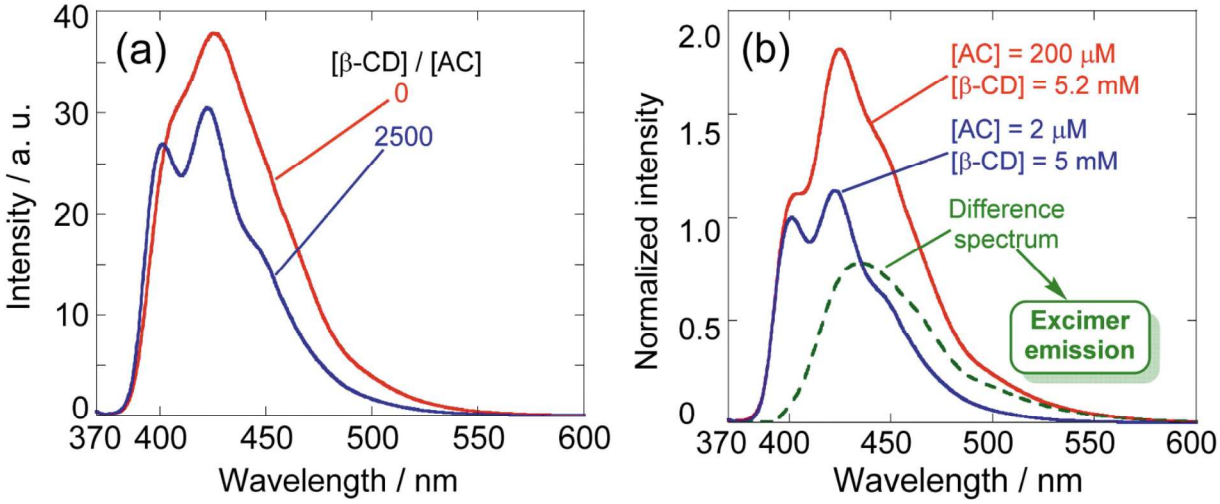

Figure 8. (a) Fluorescence spectra of AC (2 μM) in the presence (blue) and absence (red) of β-CD (5 mM) in PBS (pH 9.0) at 25 °C; λ_{ex} 327 nm. (b) Normalized (in the short wavelength region below 393 nm) fluorescence spectra of AC at 2 μM (blue) and 200 μM (red) in the presence of β-CD (5 mM) in PBS (pH 9.0) at 25 °C (λ_{ex} 327 nm) and the fluorescence spectrum of the excimer formed in the 2:2 complex, which was estimated by the spectrum subtraction of the former from the latter.

In contrast, a solution containing 100-fold more concentrated AC (200 μM) and comparable concentration of β-CD (5.2 mM) exhibited broader fluorescence with a tail extended to longer wavelengths (Figure 8b, red). The fluorescence spectra at high and low AC concentrations are normalized in the short-wavelength region and subtracted to give a difference spectrum shown in Figure 8b (green broken line), which is considered to be the excimer fluorescence from 2:2 complex, the population of which amounts to 4.8% (meaning that 9.2% of the incident light is absorbed by the dimeric species) under the conditions employed; the remainders are free AC (4.7%) and the 1:1 complex (90.5%); see Table 2. Excimer fluorescence of anthracene has rarely been observed in solution due to the rapid radiative and non-radiative decays through fluorescence and photocyclodimerization. Nevertheless, ACs tethered to a diol scaffold are known to form a frustrated excimer, which is sterically hindered from cyclodimerization and hence fluoresces at wavelengths slightly longer than the monomer emission.[22] In the present case, the photocyclodimerization is thought to be supramolecularly decelerated by confining the pair of ACs in a dual β-CD capsule.

The fluorescence excitation spectra of a 2 μM AC solution containing 5 mM β-CD monitored at 400 and 500 nm (Figure 9a) were practically superimposable with each other. In contrast, the excitation spectrum of a 200 μM AC solution with 5.2 mM β-CD monitored at 500

nm significantly deviated to longer wavelengths from that monitored at 400 nm and also from the UV-vis spectrum (Figure 9b). This is attributed to the bathochromic shift of AC (200 μM) in the UV-vis spectrum due to the partially stacked ACs in 2:2 complex (Figure 7). These results clearly indicate that the emission at longer wavelengths originates from the excitation of ground-state AC dimer partially stacked in a β-CD capsule.

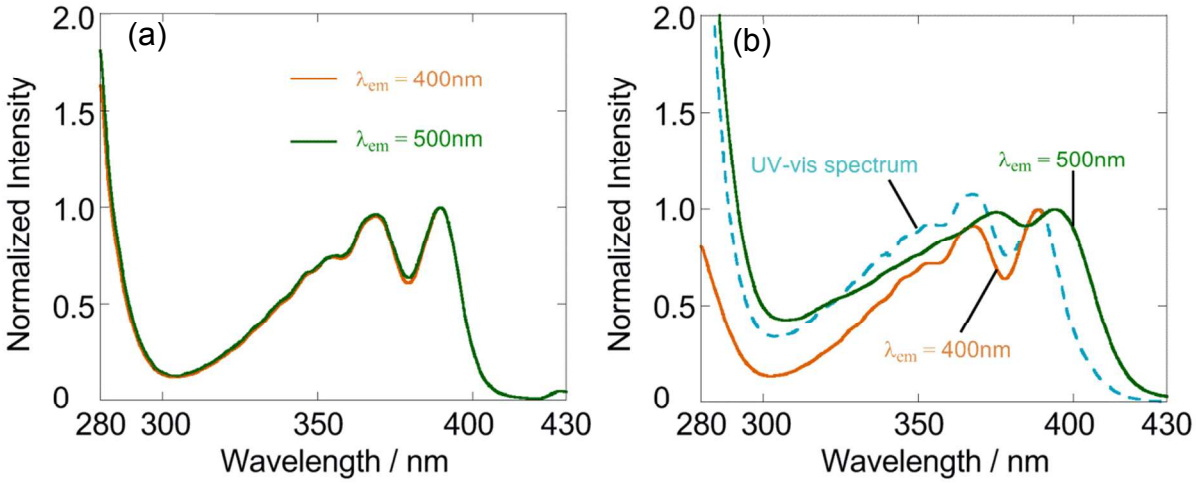

Figure 9. (a) Normalized excitation spectra of AC at 2 μM in the presence of β-CD (5.0 mM), monitored at 400 (orange) and 500 nm (green); (b) normalized excitation spectra of AC at 200 μM in the presence of β-CD (5.2 mM), monitored at 400 (orange) and 500 nm (green), and UV-vis spectrum (dotted cyan); all in PBS (pH 9) at 25 °C.

This conclusion is reinforced by the result of fluorescence lifetime measurements. AC (2 μM) in PBS gave a single fluorescence lifetime (τ_1) of 16.9 ns, irrespective of the monitoring wavelength employed (Table 2, top two lines). Upon addition of β-CD (5 mM) to this dilute AC solution, the decay profile became a sum of two exponential functions of τ_1 = 16.9 ns and τ_2 = 10.9-11.2 ns, the latter of which was assigned to the excited 1:1 complex dominating with relative abundance (A_2) of 89% at 400 nm and 68% at 500 nm. The smaller A_2 value obtained

upon monitoring at 500 nm is attributable to the sharpening of the fluorescence spectrum upon inclusion by β-CD (Figure 8a).

Table 2. Fluorescence Lifetimes of Free AC (τ_1), 1:1 Complex (τ_2), and 2:2 Complex (τ_3) Determined at Different Concentrations and Monitoring Wavelengths[a]

AC /μM	β-CD /mM	population[b]/%			λ_{em}[c] /nm	τ_1 /ns	A_1	τ_2 /ns	A_2	τ_3 /ns	A_3	χ^2
		free AC	1:1 complex	2:2 complex								
2	0	100			400	16.9						1.09
					500	16.9						1.09
2	5.0	5.00	94.95	0.05	400	16.9[d]	*0.11*	11.2	*0.89*			1.06
					500	16.9[d]	*0.32*	10.9	*0.68*			1.09
200	5.2	4.7	90.4	4.9	400	16.9[d]	*0.22*	10.4	*0.78*			1.06
					500	16.9[d]	*0.16*	10.4[d]	*0.51*	57.9	*0.33*	1.06

[a] Measured in PBS (pH 9.0) at 25 °C: λ_{ex} = 340 nm. [b] Calculated by using K_1 = 3800 M^{-1} and K_2 = 150 M^{-1} (Table 1). [c] Monitoring wavelength. [d] Fixed value.

At the higher AC concentration (200 μM), two species of τ_1 = 16.9 ns and τ_2 = 10.4 ns were similarly observed when monitored at 400 nm, but a new much longer-lived species of τ_3 = 57.9 ns emerged in addition to the above two species when the fluorescence was monitored at 500 nm (Figure 10a and Table 2, bottom lines, see also Figure S47).[15] It is to note that the decay profile was successfully analyzed without involving a rise, implying that the formation of 2:2 complex is not an excited-state but a ground-state event. As shown in Figures 10b and S48,[15] the time-resolved fluorescence spectra taken at 1, 10, 30, and 50 ns after excitation revealed that the high-energy fluorescence from the excited 1:1 complex decays rapidly to leave a long-lived broad fluorescence that resembles in shape the steady-state excimer fluorescence obtained by the spectrum subtraction (Figure 8b). We therefore assigned this red-shifted, longer-lived structureless emission to the excimer fluorescence from the slipped AC pair in a 2:2 complex.

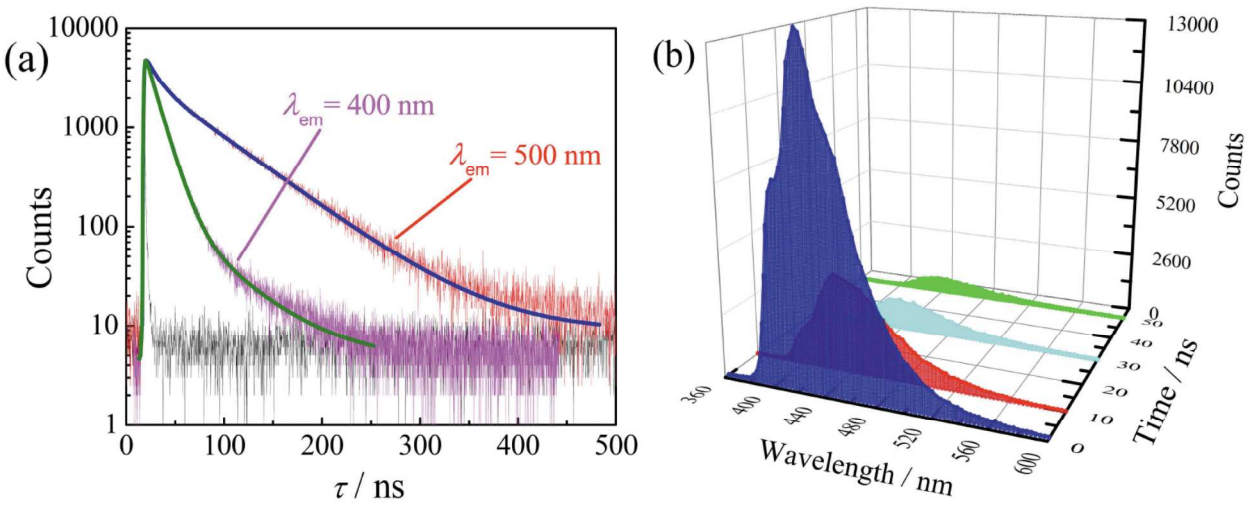

Figure 10. (a) Fluorescence decay profiles of AC (200 μM) in the presence of β-CD (5.0 mM) at 25 °C, monitored at 400 nm (purple) and 500 nm (red); λ_{ex} 280 nm. (b) Time-resolved fluorescence spectra at 1 (blue), 10 (red), 30 (cyan), and 50 ns (green) after excitation.

Upon excitation in fluid solution, anthracene derivatives usually emit monomer fluorescence or undergo photocyclodimerization, and no excimer fluorescence is observed even at low temperatures. Ferguson and coworkers, however, have demonstrated that an anthracene pair generated by photosplitting anthracene cyclodimer gives an emissive excimer in rigid matrices at 77 K.[23] Ramamurthy et al. have observed the excimer fluorescence of a pair of unsubstituted anthracenes (AN) confined in an octa acid (OA) capsule in aqueous solution at room temperature, where the photocyclodimerization is completely suppressed.[4b] The confinement of two AN molecules in a rigid OA capsule of slow assembling/disassembling dynamics and the sterically hindered photocyclodimerization in a narrow capsule are jointly responsible for this unprecedented observation of excimer fluorescence in solution.

The present excimer generated by the excitation of a 2:2 complex of AC with β-CD ([AC_2•β-CD_2]*) differs in photophysical and photochemical behavior from the AN excimer

confined in OA capsule ([AN_2•OA_2]*). Thus, the Stokes shift of excimer fluorescence is much smaller for [AC_2•β-CD_2]* than for [AN_2•OA_2]* and the lifetime is also significantly shorter for the former (60 ns) than for the latter (263 ns).[4b] More crucially, [AC_2•β-CD_2]* can cyclodimerize to regular 9,10:9',10'- and slipped 5,8:9',10'-cyclodimers (Scheme 1). All of these unusual photophysical and photochemical behaviors are attributable to the slipped arrangement of two ACs accommodated in a weakly bound dual β-CD capsule (K_2 = 150 M^{-1} at 25 °C), which allows the slipped excimer to competitively fluoresce with a small Stokes shift and cyclodimerize in both regular and irregular manners in a readily disassembling soft capsule.

Photocyclodimerization Kinetics. The overall photocyclodimerization rate was determined at 25 °C for a PBS solution of AC (0.2 mM) in the presence and absence of β-CD (2 mM) by monitoring the UV-vis spectral changes upon irradiation at 365 nm with LED. As shown in Figures S49-S52,[15] the absorbance of AC smoothly decreased with increasing irradiation time and the absorbance changes obtained in the presence and absence of β-CD were analyzed by assuming the first-order and second-order kinetics, respectively, to give apparent rate constants of k_1 = 0.0236 ± 0.0003 s^{-1} and k_2 = 117 ± 4 M^{-1} s^{-1} (or k_2[AC] = 0.0234 s^{-1} at [AC] = 0.2 mM). The apparent rate acceleration by β-CD may look essentially nil, being mere 1.01-fold, but the population of the 2:2 complex is only 4% at the host and guest concentrations employed; note that the 1:1 complex of 84% population is practically photoinert, while free AC of 12% population may undergo photocyclodimerization but its contribution to the overall rate is nearly negligible due to the bimolecular nature of the reaction. Considering this population and the fact that the 2:2 complex contains two AC molecules and hence has a twice larger absorbance than free AC, we calculated the real acceleration as 13-fold at this relatively low concentration of AC (0.2 mM). This significant acceleration well rationalizes the dominant formation of **1**, **5**, and **6** derived from the less populated 2:2 complex.

It would be interesting if the individual photocyclodimerization rate constants for *re-re*, *re-si*, and *si-si* complexes (Scheme 2) could be estimated. However, this is hampered by the lack of information about the population of these species in the solution (which should differ from the product distribution, as the rate of subsequent photocyclodimerization is not the same for each species). Nevertheless, we examined the time course of the photocyclodimerization of AC (0.2 mM) in the presence of *β*-CD (2.0 mM) at 25 °C by monitoring the UV-vis spectral changes upon irradiation for up to 75 min. The yields of cyclodimers **1**-**6** were determined every 15 min of irradiation by chiral HPLC (Figure S53).[15] The product distribution was kept constant throughout the irradiation, and the reaction obeyed the apparent first-order rate equation to give the rate constant shown in Table S5 in SI. In a solution containing 0.2 mM AC and 2.0 mM *β*-CD, there exist free AC, 1:1, and 2:2 complexes in a 12:84:4 ratio, but decoupling the contribution of *re-re, re-si,* and *si-si* complexes is not feasible and hence the individual rate constants cannot be estimated. However, this experiment enabled us to confirm that the product ratio does not vary at least up to 80% conversion, indicating the sole origin of the slipped dimers.

Diastereomeric 2:2 Complexation and Enantiomeric Photocyclodimerization Mechanisms. We first consider the stereochemical aspects of the 2:2 complexation and subsequent photocyclodimerization of the AC pair in a *β*-CD capsule. Since prochiral AC possesses the enantiotopic *re* and *si* faces, there exist four possible stereoisomeric 2:2 complexes: *re-si*, *si-re*, *re-re*, and *si-si* (Scheme 2). The former two are stereochemically equivalent to each other and photocyclodimerize either to achiral cyclodimer **1** or to chiral slipped cyclodimer **5**. It is worth mentioning that the excitation of either *re*-AC or *si*-AC in a *re-si* complex leads to distinctly different stereochemical consequences, affording either *re**-*si* or *re-si** complex, which are diastereomeric to each other. On the other hand, the latter two (i.e., the *re-re* and *si-si* complexes) are inherently diastereomeric in the ground and excited states and photocyclodimerize to the corresponding enantiomer of cyclodimer **2** or slipped cyclodimer **6**.

Scheme 2. Photocyclodimerization of Diastereomeric 2:2 Complexes to Regular 9,10:9',10'-Cyclodimers (**1** and **2**) and Slipped 5,8:9',10'-Cyclodimers (**5** and **6**) in a β-CD Capsule[a]

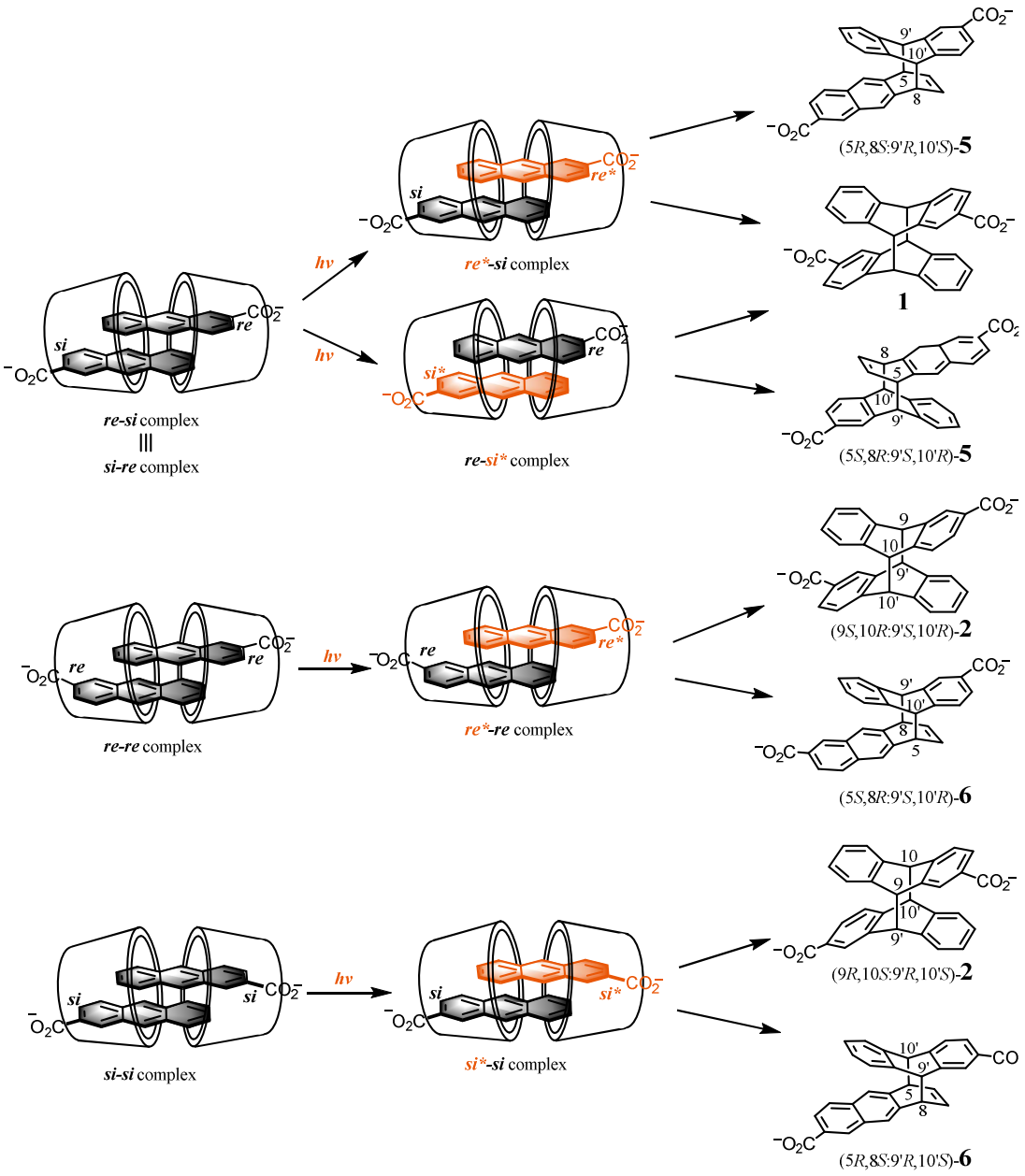

[a] *Re-si* and *si-re* complexes are equivalent to each other in the ground state but photoexcitation of *re*- or *si*-AC in a *re-si* (or *si-re*) complex breaks the centrosymmetric nature of two facing ACs to render the resulting *re**-*si* or *re-si** complex diastereomeric. On the other hand, the *re-re* and *si-si* complexes are inherently diastereomeric to each other in both ground and excited states.

As illustrated in Scheme 2 (top branching equation), when a *re-si* (or *si-re*) complex photocyclodimerizes at the 9,10-positions, achiral **1** is formed. If the photocyclodimerization occurs between the *si*-AC's 5,8-positions and the *re*-AC's 9,10-positions, slipped (5*R*,8*S*:9'*R*,10'*S*)-**5** is produced, while the reaction between the *re*-AC's 5,8-positions and the *si*-AC's 9,10-positions leads to antipodal (5*S*,8*R*:9'*S*,10'*R*)-**5**. In the case of *syn*-HT complex (Scheme 2, bottom two equations), the diastereomeric *re-re* and *si-si* complexes respectively afford enantiomeric (9*S*,10*R*:9'*S*,10'*R*)- and (9*R*,10*S*:9'*R*,10'*S*)-**2** upon 9,10:9',10'-cyclodimerization and also slipped (5*S*,8*R*:9'*S*,10'*R*)- and (5*R*,8*S*:9'*R*,10'*S*)-**6** upon 5,8:9',10'-cyclodimerization. Since neither the re-equilibration among the excited complexes nor the swapping of two ACs in the narrow cavity of a *β*-CD capsule is expected to occur within the short lifetimes (vide supra), the chemical and optical yields of each product are determined by the ground-state thermodynamics (i.e., the population of free AC and 1:1 and 2:2 complexes) and the excited-state kinetics (i.e., the photocyclodimerization efficiency of relevant complexes), both of which can be manipulated by the host/guest ratio, the excitation wavelength, and the environmental variants, such as temperature, pressure, and solvent conditions.

Enantiodifferentiating Photocyclodimerization of AC with *β*-CD: Effects of Host/Guest Ratio and Temperature. To quantitatively discuss the photochemical and stereochemical consequences of the 2:2 complexation, the effects of *β*-CD concentration and temperature on the chemical and optical yields of slipped cyclodimers **5** and **6** were first examined. Table 3 lists the population of free AC, 1:1, and 2:2 complexes in the solutions of AC (0.2 mM) in PBS (pH 9) at various *β*-CD concentrations (0-5.2 or 0-11.4 mM) and temperatures (50, 25, and 0.5 °C), and also the chemical yields and enantiomeric excesses (ee's) of regular cyclodimers **1**-**4** and slipped **5** and **6** obtained upon photoirradiation of the solutions; for the full results, see Table S3.

Table 3. Enantiodifferentiating Photocyclodimerization of AC Mediated by native β-CD in PBS at Various Host/Guest Ratios and Temperatures[a]

T/ °C	AC /mM	β-CD /mM	population[b]/%			irradiation/h	conversion[c]/%	yield/%						ee[d]/%				5/1	6/2	(1+5) /(2+6)
			free AC	1:1 complex	2:2 complex			**1**	**2**	**3**	**4**	**5**	**6**	**2**	**3**	**5**	**6**			
50	0.2	0.6	51.2	48.0	0.8	0.5	50	47	26	13	7	5	2	1	-1	40	37	0.11	0.06	1.9
		5.2	9	88	3	0.5	55	60	4	3	1	23	9	-8	-1	41	31	0.38	2.1	6.3
		11.4	5	92	3	0.5	55	61	3	2	*e*	25	9	-12	-3	37	26	0.41	3.3	7.7
25	0.2	0	100	0	0	0.5	46	40	34	16	10	0	0	0	0	*f*	*f*	0	0	1.2
		0.1	80.8	19.0	0.2	0.5	37	42	31	15	9	2	1	-1	0	46	31	0.06	0.02	1.4
		0.2	66.0	33.3	0.7	0.5	38	50	24	10	7	7	2	-1	-1	48	34	0.15	0.09	2.1
		0.6	35	63	2	0.5	43	59	8	4	3	20	6	-5	0	45	32	0.34	0.79	5.5
		5.2	5	90	5	0.5	57	65	1	1	*e*	25	8	-10	-1	47	24	0.39	6.0	9.2
0.5	0.2	0.2	53.3	45.9	0.8	0.5	39	59	10	5	4	17	5	-4	-1	43	15	0.29	0.5	5.0
		0.6	20	74	6	0.5	26	64	2	1	1	24	8	-14	-5	44	17	0.38	3.1	8.8
		5.2	2	89	9	0.5	37	65	1	*e*	*e*	26	8	-18	*g*	43	16	0.39	8.1	10.0
						2.0	95	65	1	*e*	*e*	26	8	-18	*g*	44	17	0.40	8.0	10.1
	0.6	5.2	2	78	20	0.5	42	62	*e*	*e*	*e*	29	9	-17	*g*	43	15	0.47	>20	10.6

[a] PBS solutions (pH 9.0) of AC and β-CD were irradiated at 390 nm with a 300W xenon lamp through an interference filter (bandwidth = 10 nm). [b] Calculated from the K_1 and K_2 values obtained experimentally or extrapolated by using the thermodynamic parameters in Table 1. [c] Consumption of AC determined by UV-vis monitoring at 388 nm. [d] Enantiomeric excess determined by chiral HPLC, where the first-eluted enantiomer is given a positive sign for all of the chiral products, i.e., **2**, **3**, **5**, and **6**; error in ee < 2%. [e] Yield < 0.5%. [f] Not applicable. [g] Not determined due to low yield.

In the absence of *β*-CD, the photoirradiation of AC (0.2 mM) for 30 min at 25 °C led to a 46% conversion and the dominant formation of **1** and **2** in 74% combined yield. This HT-preference is attributable to the electrostatic and steric repulsions of the carboxylate anions in two reacting ACs. Notably, no irregular dimers were detected. Upon addition of 0.1-5.2 mM *β*-CD at 25 °C, the conversion of AC was first reduced to 37% at 0.1 mM *β*-CD but then gradually increased to reach 57% at the highest host concentration. The initial reduction and the rather slow growth of conversion thereafter are sensible, since the 1:1 complexation with *β*-CD blocks the photocyclodimerization of included AC. It should be noted however that even a substoichiometric amount of *β*-CD (0.1 mM), with the population of 2:2 complex at mere 0.2% (Table 3), is sufficient to turn on the slipped photocyclodimerization to **5** and **6** and their ee's are comparable to those obtained at higher host concentrations, indicating the catalytic nature of the higher-order complex. Thus, under the condition of $K_2 < K_1$, the system can be catalytic because the dissociation is likely to be faster for the weakly bound 2:2 complex than for the stronger 1:1 complex, enabling the latter to serve as a reservoir for the catalytic precursor complex, while the release of the volume-expanded product cyclodimer from the *β*-CD capsule should be spontaneous. Such a situation will enhance the turnover of the catalytic cycle.

The chemical yield change was more straightforward as a function of host concentration. When the concentration of *β*-CD was increased to 5.2 mM, cyclodimers **2**-**4** almost disappeared and **1**, **5**, and **6** became dominant (98% combined yield at 57% conversion). This dramatic switching of product selectivity, as well as the gradually increasing conversions mentioned above, are directly related to the enhanced population of 2:2 complex, which is still low (5%) even at the highest host concentration but greatly expedites the subsequent photocyclodimerization to dominate the overall photochemistry. Since both **1** and **5** are derived

from the *anti*-HT (*re-si* and *si-re*) complexes while **2** and **6** from the *syn*-HT (*re-re* and *si-si*) complexes (Scheme 2), the *anti/syn* preference upon complexation and photocyclodimerization can be evaluated by the (**1**+**5**)/(**2**+**6**) ratio. As shown in Table 3, the *anti/syn* preference rapidly increases from 1.2 to 9.2 as the concentration of *β*-CD increases from 0 to 5.2 mM. The thermodynamically favored *anti*-HT complexation and the kinetically expedited photocyclodimerization are most likely responsible for this trend. In contrast, the **5**/**6** ratio is kept constant at around 3 over the entire concentration range employed, indicating the single origin, i.e. the 2:2 complex. It is also interesting that the *anti*-HT complex favors the photocyclodimerization to regular 9,10:9',10'-cyclodimer **1** with a **5**/**1** ratio of 0.39 at 5.2 mM *β*-CD, whereas the *syn*-HT complex predominantly photocyclodimerizes to **6** with a **6**/**2** ratio of 6.0 at the highest *β*-CD concentration. This is probably because the *syn*-HT complexation is inherently less favored (as judged from the (**1**+**5**)/(**2**+**6**) ratio as high as 9.2) and the 9,10:9',10'-photocyclodimerization of two ACs in the *syn*-HT complex, requiring deeper mutual penetration into the *β*-CD cavity, is sterically more demanding and less favored.

The enantiomeric excess (ee) of **2** was consistently low (<10%) at 25 °C, while those of slipped cyclodimers **5** and **6** were much higher at 43-48% and 24-34%, respectively. More crucially, the ee values for **5** and **6** did not vary with the host or AC concentration or the irradiation time of up to 2 h to achieve a 95% conversion (Table 3), supporting the above conclusion that the slipped cyclodimers originate solely from the 2:2 complex. The crucial role of photocyclodimerization kinetics was revealed by the inconsistent ee values obtained for **2** versus **6**. If the diastereomeric *re-re* and *si-si* complexes spontaneously cyclodimerized upon irradiation at the same rate, the ee's of the cyclodimers would be determined exclusively by the ground-state population of the *re-re* and *si-si* complexes (Scheme 2). Also, the ee's of **2** and **6**

should be identical to each other, but they significantly differ in reality (Table 3). This difference in ee is accounted for only by the unequal cyclodimerization rates for the diastereomeric precursor complex pair, while the slowly reacting species can emit excimer fluorescence (Figure 8). Similarly, the *re-si* and *si-re* complexes may photocyclodimerize to **1** and **5** at different rates. However, the fact that the **5**/**1** ratio and the ee of **5** at high β-CD concentrations do not show any appreciable dependence on temperature implies that the precursor complexes spontaneously cyclodimerize upon excitation without emitting light, and the **5**/**1** ratio and the ee of **5** reflect the ground-state population. If so, the excimer fluorescence observed could be ascribed solely to the less-reactive *syn*-HT complex.

We further examined the effects of AC concentration at 0.5 °C, while keeping the β-CD concentration at 5.2 mM; the results are shown in Tables 3 and S3.[15] By increasing the AC concentration from 0.2 to 0.6 mM, the initial population of 2:2 complex was enhanced from 9% to 20% and accordingly the conversion augmented from 37% to 42% and the combined yield of slipped dimers **5** and **6** from 34% to 38%, while the ee values of **5** and **6** were kept unchanged, reinforcing our claim that they arise solely from the 2:2 complex. The augmentation of conversion from 37% at 0.2 mM to 42% at 0.6 mM is apparently much smaller than the 2.2-fold enhancement of the population of 2:2 complex (from 9% to 20%), but is actually equivalent to a 3.3-fold enhancement in net mole quantity of the consumed AC. The greater enhancement in conversion than in population is sensible, because the population of 2:2 complex is not invariable but rapidly decreases with lowering AC concentration as the photocyclodimerization proceeds.

Wavelength Effects. Altering excitation wavelength is a convenient yet powerful tool for controlling the stereochemical consequence of photoreaction, particularly when multiple supramolecular complex species are involved. Indeed, the photocyclodimerization of AC

mediated by γ-CD is known to display significant excitation-wavelength effects, affording varying ee's for **2** and **3** upon irradiation at different wavelengths.[24] In the present system (Scheme 2), two sets of diastereomeric 2:2 complexes, i.e. *re-si/si-re* and *re-re/si-si* pairs, are involved. If these complexes differ in absorption spectrum, the distribution and ee of cyclodimers are expected to vary with irradiation wavelength.

PBS solutions containing AC (0.2 mM) and β-CD (4.4 mM) were irradiated at different wavelengths; the excitation at short wavelengths below 350 nm was not effective due to the photoreversion of the slipped cyclodimers produced. By changing the excitation wavelength from 360 nm to 410 nm, the **5**/**1** ratio was slightly increased from 0.35 to 0.38, whereas the **6**/**2** ratio was doubled from 1.5 to 3.0 (Table 4; see also Table S4). The enantioselectivity exhibited similar wavelength-dependent behaviors, affording nearly constant ee values of 45-47% for **5** but more variable ee's fluctuating from 31% to 40% with a maximum at 380 nm for **6**. These results indicate that the *re-si* and *si-re* complexes behave very similarly but the *re-re* and *si-si* complexes appreciably differ in spectroscopic properties and photoreactivity.

Table 4. Photocyclodimerization of AC Mediated by Native and Ammonio- and Guanidino-Modified β-CDs in PBS at Various Wavelength (λ), Temperature (T), and Pressure (P) in the Presence and Absence of Inorganic Salt[a]

host	conc. /mM	AC /mM	λ/nm	P /MPa	added salt	conc. /M	T /°C	conver-sion/%	yield/%						ee[b]/%				**5**/**1**	**6**/**2**	(**1**+**5**)/ (**2**+**6**)
									1	**2**	**3**	**4**	**5**	**6**	**2**	**3**	**5**	**6**			
β-CD	4.4	0.2	360[c]	0.1	none	0	25	36	63	5	2	1	22	7	-4	-1	47	34	0.35	1.5	7.3
			410[c]	0.1	none	0	25	29	64	3	1	*d*	25	8	-3	1	46	31	0.38	3.0	8.7
	5.2	0.2	390[c,e]	0.1	none	0	25	78	61	1	1	*d*	28	9	-11	-5	44	21	0.45	6.8	8.0
				385	none	0	25	85	72	5	*d*	*d*	13	10	-30	*f*	42	15	0.18	1.8	5.6
			390[c]	0.1	none	0	25	57	65	1	1	*d*	25	8	-10	-1	47	24	0.38	6	10.0
					NH_4Cl	1.0	25	37	69	3	1	*d*	20	6	-9	-15	43	30	0.29	2	9.9
					$MgCl_2$	1.0	25	43	53	1	*d*	*d*	34	11	-22	*f*	45	21	0.64	10	7.3
					LiCl	1.0	25	43	60	1	1	*d*	29	9	-14	-10	45	30	0.48	7	8.9
						4.2	25	45	45	1	*d*	*d*	41	13	-19	*f*	48	24	0.91	15	6.1
							-15	21	40	1	*d*	*d*	46	13	-19	*f*	44	21	1.15	11	6.1
					CsCl	1.0	25	54	60	1	1	*d*	29	9	-11	-8	41	32	0.48	6	8.9
						6.0	40	44	16	*d*	*d*	*d*	59	25	*f*	*f*	32	10	3.8	*g*	2.9
							-20	25	20	*d*	*d*	*d*	49	31	*f*	*f*	-7	-36	2.5	*g*	2.2
7	5.2	0.2	365[h]	0.1	CsCl	6.0	40	33	5	*d*	*d*	*d*	67	28	*f*	*f*	39	14	13	*g*	2.6
							-20	17	1	*d*	*d*	*d*	66	33	*f*	*f*	22	-18	47	*g*	2.1
8	5.2	0.2	365[h]	0.1	CsCl	6.0	40	32	17	*d*	*d*	*d*	55	28	*f*	*f*	30	5	3.3	*g*	2.6
							-20	49	7	*d*	*d*	*d*	48	45	*f*	*f*	-1	-44	6.9	*g*	1.2
9	5.2	0.2	365[h]	0.1	CsCl	6.0	40	39	31	*d*	*d*	*d*	46	23	*f*	*f*	30	14	1.5	*g*	3.3
							-20	53	8	*d*	*d*	*d*	56	36	*f*	*f*	-10	-32	6.5	*g*	1.8
10	5.2	0.2	365[h]	0.1	CsCl	6.0	40	30	5	*d*	*d*	*d*	58	37	*f*	*f*	33	5	11	*g*	1.7
							-20	47	3	*d*	*d*	*d*	50	47	*f*	*f*	5	-45	18	*g*	1.1
11	0.5	0.6	365[h]	0.1	none	0	25	82	3	2	1	*d*	80	14	0	*f*	56	8	23	7.4	5.3
					CsCl	6.0	25	38	1	*d*	*d*	*d*	84	15	*f*	*f*	65	-7	154	*g*	5.7
	5.2	0.2	365[h]	0.1	CsCl	6.0	40	29	*d*	*d*	*d*	*d*	80	20	*f*	*f*	71	-8	800	*g*	4.0
							-20	49	*d*	*d*	*d*	*d*	85	15	*f*	*f*	52	-17	*g*	*g*	5.6
12	5.2	0.2	365[h]	0.1	CsCl	6.0	40	28	1	*d*	*d*	*d*	49	50	*f*	*f*	18	33	44	*g*	1.0
							-20	51	*d*	*d*	*d*	*d*	64	36	*f*	*f*	-30	19	640	*g*	1.8

[a] Irradiation performed for 30 min in a cryostat under the conditions comparable to those shown in Table 3, unless noted otherwise. For the full results, see Table S4. b Enantiomeric excess determined by chiral HPLC, where the first-eluted is given a positive sign for all of the chiral prodcuts, i.e., **2**, **3**, **5**, and **6**; error in ee <2%. [c] Irradiated for 30 min with monochromatic light from a 300-W xenon lamp fitted with an appropriate interference filter (fwhm = 10 nm). [d] Yield <0.5%. [e] Performed in a pressure vessel, and hence the conversion cannot be compared with the other data. [f] Not determined due to the low yield. [g] Larger than 1000 due to the low yield of **1** or **2**. [h] Irradiated at 365 nm with LED for 30 min.

Pressure Effects. Hydrostatic pressure is a unique tool for controlling the rate and equilibrium of chemical process through the volume difference of relevant species and/or transition states.[25] Thus, the process with a smaller activation or reaction volume is facilitated under elevated pressures. We have demonstrated that the chemical and optical yields are critically affected by applying high pressure in the diastereodifferentiating photocyclodimerization of α-CD-appended AC mediated by γ-CD.[13e,26] In the present system, if the *re-si/si-re* and *re-re/si-si* complexes, as well as the transition states to regular 9,10:9',10'-cyclodimers and slipped 5,8:9',10'-cyclodimers, were not exactly the same in volume, the product distribution and enantioselectivity should be influenced by pressure.

The photocyclodimerization of AC (0.2 mM) was performed in the presence of β-CD (5.2 mM) under a pressure of 385 MPa, and the result was compared with that obtained under atmospheric pressure. As shown in Table 4, the conversion was appreciably increased from 78% to 85% by applying pressure, indicating that the 1:1 and 2:2 complexation and/or the photocyclodimerization in the latter complex are facilitated under higher pressure. The product distribution and ee suffered much larger effects. Thus, the yields of regular cyclodimers **1** and **2** were greatly enhanced at the expense of slipped cyclodimer **5**, while the yield of **6** was slightly increased, leading to significantly decreased **5**/**1** and **6**/**2** ratios by a factor of 2.5 and 3.8, respectively, when compared with the corresponding ratios obtained at atmospheric pressure. Since the branching to regular and slipped cyclodimerization occurs upon photoexcitation, these results indicate that the transition states to regular cyclodimers are considerably more compact than those to the corresponding slipped cyclodimers. This seems reasonable as the formation of the regular cyclodimer requires further mutual penetration of the two slipped HT-oriented ACs into the β-CD cavity with accompanying reduction of the total volume in the transition state.

The mechanism that determines the ee's of **2**, **5**, and **6** is more complicated, being governed dually by the ground-state equilibria and the excited-state kinetics. As can be seen from Scheme 2, the ee of **5** is determined by the population and relative photocyclodimerization rate of *re-si* and *si-re* complexes, while the ee's of **2** and **6** by those of *re-re* and *si-si* complexes. Therefore, each ee may behave differently under high pressure. Indeed, the ee of **2** was greatly enhanced from -11% to -30% by applying pressure of 385 MPa, while those of **5** and **6** more or less decreased under the elevated pressure. These changes, however, cannot be attributed to a single cause or step as they originate from the combined effects of pressure on the complexation equilibria and the photocyclodimerization rates.

Salt Effects. The salt effects on the photocyclodimerization of AC (0.2 mM) mediated by *β*-CD (5.2 mM) were first examined at 25 °C. As shown in Tables 4 (see also Table S4),[15] the conversion was appreciably reduced from 57% to 37-54% upon addition of 1 M salt, while the yield and ee were less affected for the major products (**1** and **5**) but noticeably enhanced for the minor products (**2** and **6**).

The salt effects became more evident at higher salt concentrations and in particular at lower temperatures. In the presence of 4.2 M LiCl, the conversion was reduced to 45% and the chemical yields of **5** and **6** increased from 25% and 8% to 41% and 13%, respectively, at 25 °C. On the other hand, the ee of **2** was only modestly improved and those of **5** and **6** almost unaffected. Lowering the temperature to –15 °C further decreased the conversion to 21% and enhanced the relative yield of **5**, but slightly reduced the ee's of **5** and **6**. Upon addition of 6 M CsCl (which was incapable of inducing any Lewis acid-initiated thermal transformation of AC),[15] the irregular 5,8:9',10'-photocyclodimerization was highly favored to give slipped

cyclodimers **5** and **6** in an combined yield of 87% at 20 °C, while their ee's were reduced from 47% and 24% in 25 mM PBS at 25 °C to 23% and –4% (the positive/negative signs for ee are tentative tags for the opposite enantiomers; for the absolute configurations, see Figure 4 and the relevant discussion) in aqueous 6 M CsCl solution at 20 °C. In sharp contrast to the results in 4.2 M LiCl solution discussed above, the ee's of **5** and **6** were critically affected by temperature, leading to a switching of the product chirality between 40 °C and -20 °C. This also contrasts dramatically to the much less pronounced temperature-dependence of the ee's of **5** and **6** observed in PBS and in 4.2 M LiCl solution, suggesting that some mechanism other than the simple salting-out effect is responsible for the change in 6 M CsCl solution.

The reduced conversion and the preference for the slipped cyclodimers in the presence of concentrated salts are rationalized by the electrostatic interactions of the metal cation with the AC's carboxylate anion located near the portals of *β*-CD capsule, which should move ACs in a capsule towards each portal, forcing a more slipped (less overlapped) conformation to discourage the classical 9,10:9',10'-cyclodimerization, as illustrated in Scheme S1b.[15] This explanation is experimentally supported, as the induced circular dichroism intensity was reduced upon addition of 6 M CsCl to a solution of AC (0.2 mM) and *β*-CD (2 mM) at 25 °C (Figure S54),[15] suggesting shallower inclusion of AC in the *β*-CD cavity. In this relation, it is to note that chloride ion is weakly bound to *β*-CD,[27] which could hinder the complexation of AC. However, as shown in Table 1, the addition of 6 M CsCl did not reduce but enhanced the K_1 and K_2 values by a factor of 1.5-2, apparently indicating that the salting-out effect exceeds the influence of chloride complexation, probably due to the much higher hydrophobicity of AC. The ion-pairing interaction should be stronger for weakly hydrated Cs^+ (the Gibbs free energy of hydration: ΔG_h

= –258 kJ mol^{-1})[28] than for strongly hydrated Li^+ (ΔG_h = –481 kJ mol^{-1}),[28] particularly at lower temperatures, and differ in magnitude between the *re-si* and *si-re* complexes and between the *re-re* and *si-si* complexes, leading to the inversion of product chirality by temperature in the presence of 6 M CsCl.

The external heavy-atom effect may also be responsible for the observed dramatic temperature dependence of ee, specifically upon addition of CsCl, since the quenching of excited 2:2 complexes by Cs^+ can be diastereoselective.[29] Indeed, CsCl dynamically quenched the AC fluorescence to give considerably reduced intensities (F/F_0 = 0.60 at 0.5 M and 0.17 at 6 M) (Figure S55)[15] and comparably shorter lifetimes (τ/τ_0 = 0.60 at 0.5 M and 0.19 at 6 M) (Figure S57 and Table S5).[15] Stern-Volmer plots of the F_0/F and τ_0/τvalues against the CsCl concentration gave a straight line (Figure S58),[15] from the slope of which the quenching rate constant by CsCl was evaluated as 4 x 10^7 M^{-1} s^{-1}, a value far below the diffusion limited rate (k_{diff} = 7.4 x 10^9 M^{-1} s^{-1}).[30] In contrast, the lifetimes of the excited 1:1 and 2:2 complexes formed in a solution of 0.2 mM AC and 5.2 mM β-CD (Figures S59-S62 and Table S6)[15] were less effectively shortened upon addition of CsCl, exhibiting τ/τ_0 = 0.87 for 1:1 complex and 0.79 for 2:2 complex even at 6 M, due to the protection by CD walls; for the steady-state fluorescence quenching of 2 μM AC by 5 mM β-CD and of 200 μM AC by 5.2 mM β-CD, see Figures S63-S66.[15] The k_q values estimated by the Stern-Volmer treatment of the lifetime data at [CsCl] = 0 and 6 M are 4 x 10^6 and 7 x 10^5 M^{-1} s^{-1} for the 1:1 and 2:2 complex, respectively. These rate constants are one and two orders of magnitude slower than that for free AC (5 x 10^7 M^{-1} s^{-1}), revealing the effective protection by CD walls, in particular for the 2:2 complex.

Host Modification. The partial stacking of two ACs in a 2:2 complex rests on a critical balance between the hydrophobic interaction and the steric restriction in the narrow space. By further pulling out the included AC from the primary rim of *β*-CD, more slipped conformations are expected to be achieved to eventually enhance the chemical and optical yields of irregular photocyclodimerization (Scheme 2). We envisaged that the AC's carboxylate anion can be used as a built-in handle to manipulate the stacking conformation through electrostatic interaction. For this purpose, we synthesized a series of *β*-CD derivatives **7**-**12** that carry cationic substituent(s) on the primary rim for facilitating more slipped stacking (Scheme 1).

Prior to the photochemical study using these *β*-CD derivatives**,** we performed the calorimetric titration of AC with host **11** (as a representative cationic host) to examine whether the cationic *β*-CD also forms the 1:1 and 2:2 complexes stepwise and, if so, to what extent the cationic substituent introduced to *β*-CD can improve the association constants. The calorimetric titration performed in aqueous solution at 25 °C revealed that AC and **11** also form the 1:1 and 2:2 complexes with stepwise association constants of $K_1 = 33100\ M^{-1}$ and $K_2 = 1480\ M^{-1}$ (Figure S67),[15] which are much larger than those for native *β*-CD ($K_1 = 3800\ M^{-1}$, $K_2 = 150\ M^{-1}$), most probably due to the electrostatic interaction between the CD's cationic substituents and the AC's carboxylate anion. These association constants should significantly improve the population of 2:2 complex. For example, the population of free AC, 1:1, and 2:2 complexes in a solution containing 0.2 mM AC and 2.0 mM host is 12:84:4 for native *β*-CD (Table 3) but is greatly shifted to 1:70:29 for **11** to facilitate the subsequent photocyclodimerization.

Photolyses of AC in the presence of cationic hosts **7**-**12** were carried out in aqueous 6 M CsCl solution at temperatures ranging from +40 to -20 °C to afford the slipped cyclodimers in much enhanced, or even perfect, selectivities, regardless of the type and number of cationic substituent(s) introduced. As shown in Table 4 (see also Table S4),[15] all of the modified *β*-CDs afforded slipped cyclodimers **5** and **6** as dominant products in 92-100% combined yield at -20 °C, while regular cyclodimer **1** (originally the major product without added salt or host modification) was dramatically suppressed to 0-8% yield and **2**-**4** were totally quenched. It is to note that pyridylmethylammonio(PMA)-*β*-CD **7** and diammonio(A_2)-*β*-CDs **10**-**12** are obviously more efficient in driving this selectivity shift to the slipped cyclodimers than simple ammonio(A)- and guanidino(G)-*β*-CDs **8** and **9**. In particular, 6^A,6^C-bis(trimethylammonio)-*β*-CD (TMA_2-*β*-CD) **11** leads to the exclusive formation of the slipped cyclodimers at all the temperatures examined, affording the highest yield of **5** in 80-85%. The electrostatic origin of this selectivity shift (illustrated in Scheme S1)[15] is supported by the fact that the more hydrophobic PMA- and TMA_2-modified *β*-CDs (**7** and **11**), rather than the parent A- and A_2-*β*-CDs (**8** and **10**), give the slipped cyclodimers in appreciably better yields, since the electrostatic attraction is inversely proportional to the dielectric constant of (local) medium.[31]

In contrast, the enantioselectivity turned out to be a critical function of the type and number of the cationic substituent introduced (Tables 4 and S4).[15] This means that the electrostatic interaction can manipulate not only the slipped conformation but also the relative stability/reactivity of the diastereomeric precursor complex pairs. Nevertheless, the ee's of slipped cyclodimers **5** and **6** did not greatly exceed those obtained with native *β*-CD in the presence of salt, revealing the difficulty to precisely control the enantiotopic face selectivity of

AC in the 2:2 complex with *β*-CD. The only exception was the ee of **5** obtained upon irradiation with $6^A,6^C$-TMA_2-*β*-CD **11**, which was 52% at -20 °C but reached 71% at 40 °C. In contrast, regioisomeric $6^A,6^D$-TMA_2-*β*-CD **12** gave much lower ee's for **5**, demonstrating the pivotal role of the (relative) position of cationic substituents on the rim.

We have already shown above that the present supramolecular photochirogenesis proceeds "catalytically" in a sense that the otherwise-inaccessible route to slipped cyclodimers is switched on by native *β*-CD (0.1 mM) added as a catalyst, which is substoichiometric in quantity against substrate AC (0.2 mM). Nevertheless, the substoichiometric quantity is not enough to completely suppress the photocyclodimerization of free AC remaining in the solution. The situation is however greatly improved by employing cationic *β*-CD host **11**, which exhibits one order of magnitude larger association constants for AC (K_1 = 33100 M^{-1}, K_2 = 1480 M^{-1}) than native *β*-CD (K_1 = 3800 M^{-1}, K_2 = 150 M^{-1}) in aqueous solution at 25 °C, and hence the population of free AC, 1:1, and 2:2 complexes becomes 25:43:32 under a substoichiometric condition of 0.5 mM host **11** and 0.6 mM AC (Figure S67).[15] This solution was subjected to the photoirradiation at 25 °C to obtain regular cyclodimers **1**-**4** in mere 5% combined yield and slipped cyclodimers **5** and **6** in 95% combined yield with 56% and 8% ee, respectively, as shown in Table 4. Addition of 6 M CsCl further augmented the K_1 value to 49900 M^{-1} and the K_2 value to 3090 M^{-1} to shift the population of free AC, 1:1, and 2:2 complexes up to 22:34:44 (Figure S67),[15] which eventually enhanced the combined yield of slipped cyclodimers up to 99% (**5**:**6** = 85:14) to achieve the undisputable supramolecular photocatalysis with an improved 65% ee for **5** and an sign-inverted -7% ee for **6**.

SUMMARY AND CONCLUSIONS

The new findings obtained in the present study by scrutinizing the sophisticated complexation and photocyclodimerization behaviors of AC with native and modified β-CDs are summarized:

(1) AC forms not only the 1:1 complex with β-CD at K_1 = 3800 M^{-1}, but also the unconventional 2:2 complex at K_2 = 150 M^{-1} (at 25 °C);

(2) In the 2:2 complex, two ACs are partially stacked to each other exclusively in a head-to-tail manner at the far-end of AC in a capsule composed of two β-CDs associated at the secondary rim;

(3) Formations of the 1:1 and 2:2 complexes are driven by the enthalpic gains ($-\Delta H°$) of 22.6 and 16.5 kJ mol^{-1}, respectively, with much smaller entropic losses ($T\Delta S°$) of –2.2 and –4.1 kJ mol^{-1} (at 25 °C);

(4) Upon photoexcitation, the AC pair in slipped conformation in the 2:2 complex affords a frustrated excimer that fluoresces (τ_3 57.9 ns) at wavelengths slightly red-shifted from the monomer fluorescence (τ_1 16.9 ns) due to the partial overlap at the far-end of AC;

(5) Photoirradiation of AC with β-CD preferentially affords slipped *anti*- and *syn*-HT-5,8:9',10'-cyclodimers (**5** and **6**) rather than conventional *anti*- and *syn*-HT-9,10:9',10'-cyclodimers (**1** and **2**);

(6) Both of the slipped cyclodimers are chiral and their absolute configurations are unequivocally determined by comparing the experimental versus theoretical circular dichroism spectra;

(7) The product distribution and the enantioselectivity are critical functions of temperature, pressure, salt concentration, and host modification to quantitatively afford the slipped cyclodimers in up to 71% ee for **5** and -45% ee for **6**.

It is of particular significance that a new photochirogenic route is activated in the present AC–*β*-CD system not by substrate modification but supramolecularly through the higher-order complexation. This is in keen contrast to the foregoing cases, in most of which supramolecular interactions merely modulate the rate and selectivity of existing thermodynamically and kinetically allowed process. Thus, *β*-CD (even at a substoichiometric concentration) triggers the otherwise-inaccessible nonclassical route to slipped cyclodimers by pre-organizing two AC molecules in a dual *β*-CD capsule by conformationally discouraging the conventional route to regular cyclodimers. This mechanism formally resembles the one operative in catalytic antibody, where substrate molecule(s) pre-organized in the transition state-shaped hydrophobic site of protein through multiple noncovalent interactions enjoy great acceleration in the reaction to follow.[32] In the present system, the classical route is poisoned not only by the slipped conformation of the AC pair in the capsule but also by the entrapment of AC in the 1:1 complex, which is practically photoinert but functions as a reservoir to supply the 2:2 complex when consumed, while the photoreactivity is greatly enhanced in the 2:2 complex to dominate the photochirogenic process. The *β*-CD capsule containing two AC molecules should disassemble immediately upon the volume-expanding photocyclodimerization, but is smoothly regenerated

for the repeated use through the dimerization of 1:1 complex. We may therefore regard this supramolecular organophotocatalytic system as a photochemical version of catalytic antibody, where the photocatalyst(enzyme)-substrate complex does not spontaneously react but needs photoexcitation to give the product; the only difference is the necessity for photon instead of thermal activation; see Scheme 3. However, this is not a drawback but rather an advantage as we gain additional tools for controlling chemo/regio/stereoselectivities, such as selective excitation of specific chromophoric substrate or substrate's chromophore by choosing irradiation wavelength and a very wide temperature range applicable. An essential difference from the foregoing photochirogeneses mediated by chiral supramolecular hosts is the intervention of photoinert 1:1 complex that functions as a reservoir for the photoreactive 2:2 complex, while preventing the direct non-stereoselective photocyclodimerization of free AC. It is also to note that this strategy does not require the spectral shift upon complexation, which is often used for selectively exciting the complexed substrate at the absorption edge, and hence is potentially more widely applicable.

This idea is not restricted to the present AC-CD system but potentially expandable to a wide variety of supramolecular and biomolecular systems for triggering novel reaction pathways. More practically, such a system should involve: (1) a thermal pre-equilibrium to afford a photoreactive precursor complex, in which the substrate(s) are conformationally frustrated in the binding pocket/reaction site to facilitate the subsequent photochemical transformation, (2) a photoinert reservoir/intermediate complex in dynamic equilibria with the substrate as well as the photoreactive complex to smoothly supply the latter from the former when consumed by photoreaction and also to avoid the direct non-stereoselective pathway to the product, (3) an association constant for the reservoir complex much larger than that for the photoreactive

complex for higher turnover number, and (4) spontaneous release of photoproduct from the binding pocket/reaction site to prevent the product inhibition.

Scheme 3. A Schemematic Illustration of Catalytic Supramoleculaar Photochirogenesis via Photoinert 1:1 and Photoreactive 2:2 Complexes of AC with *β*-CD, where the Spontaneous Relerease of Photoproduct (P) Prevents the Product Inhibition in this Photochemical Catalytic Antibody Mimick

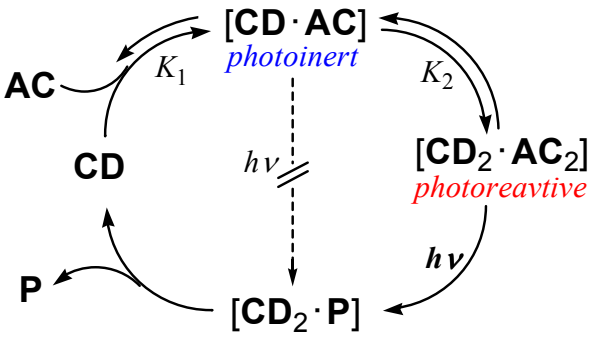

Supporting information. Experimental details, theoretical calculation method, characterization of irregular cyclodimers, supplementary photoreaction results, and the results of UV-vis, NMR, fluorescence, and circular dichroism spectroscopic, fluorescence lifetime, calorimetric titrations studies.

ACKNOWLEDGEMENT

This work was supported by the grants from the National Natural Science Foundation of China (No. 21572142, 21372165, 21321061, and 21402129) and National Key Research and Development Program of China (No. 2017YFA0505900) for CY and also by Grant-in-Aids for Scientific Research, Challenging Exploratory Research, Promotion of Joint International Research (Fostering Joint International Research), and Innovative Area "Photosynergetics" (No.

JP15H03779, JP15K13642, JP16KK0111, and JP17H05261) all from Japan Society for the Promotion of Science, Asahi Glass Foundation, and Cosmetology Research Foundation for TM, all of which are gratefully acknowledged. CY is grateful to Prof. Peng Wu and Huiqin Sun for the analyses at the Analytical and Testing Center, Sichuan University,

REFERENCES

(1) (a) Inoue, Y.; Ramamurthy, V. Eds.; *Chiral Photochemistry*; Marcel Dekker: New York, 2004. (b) Ramamurthy, V.; Inoue, Y., Eds.; *Supramolecular Photochemistry*; Wiley: Hoboken, 2011. (c) Turro, N. J.; Ramamurthy, V.; Scaiano, J. C. *Principles of Molecular Photochemistry: An Introduction*; University Science Books: Sausalito, CA, 2009. (d) Griesbeck, A. G.; Oelgemöller, M.; Ghetti, F. Eds.; *CRC Handbook of Organic Photochemistry and Photobiology*; CRC Press: Boca Raton, 2012.

(2) (a) Vallavoju, N.; Sivaguru, J. *Chem. Soc. Rev*. **2014**, *43*, 4084. (b) Yang, C.; Inoue, Y. *Chem. Soc. Rev.* **2014**, *43*, 4123. (c) Brimioulle, R.; Lenhart, D.; Maturi, M. M.; Bach, T. *Angew. Chem. Int. Ed.* **2015**, *54*, 3872. (d) Ramamurthy, V.; Gupta, S. *Chem. Soc. Rev.* **2015**, *44*, 2904. (e) You, L.; Zha, D.; Anslyn, E. V. *Chem. Rev.* **2015**, *115*, 7840. (f) Poplata, S.; Tröster, A.; Zou, Y.-Q.; Bach, T. *Chem. Rev.* **2016**, *115*, 9748. (g) Ramamurthy, V.; Sivaguru, N. *Chem. Rev.* **2016**, *115*, 9914.

(3) (a) Breslow, R.; Dong, S. D. *Chem. Rev.* **1998**, *98*, 1997. (b) V. P. Rao; N. J. Turro *Tetrahedron Lett.* **1989**, *30*, 4641. (c) Inoue, Y.; Dong, S. F.; Yamamoto, K.; Tong, L.-H.; Tsuneishi, H.; Hakushi, T.; Tai, A. *J. Am. Chem. Soc.* **1995**, *113*, 2793. (d) Ueno, A.; Kuwabara, T.; Nakamura, A.; Toda, F. *Nature* **1992**, *356*, 136. (e) Koodanjeri, S.; Joy, A.; Ramamurthy, V. *Tetrahedron* **2000**, *56*, 7003. (f) Luo, L.; Liao, G. H.; Wu, X. L.; Lei, L.; Tung, C. H.; Wu, L. Z. *J. Org. Chem.* **2009**, *74*, 3506. (g) Yan, Z.; Huang, Q.; Liang, W.; Yu, X.; Zhou, D.; Wu, W.; Chruma, J. J.; Yang, C. *Org. Lett.* **2017**, 19, 898.

(4) (a) Biros, S. M.; Rebek Jr, J. *Chem. Soc. Rev.* **2007**, *36*, 93. (b) Kaanumalle, L. S.; Gibb, C. L.; Gibb, B. C.; Ramamurthy, V. *J. Am. Chem. Soc.* **2005**, *127*, 3674. (c) Gui, J.-C.; Yan, Z.-Q.; Peng, Y.; Yi, J.-G.; Zhou, D.-Y.; Su, D.; Zhong, Z.-H.; Gao, G.-W.; Wu, W.-H.; Yang, C. *Chin. Chem. Lett.* **2016**, 27, 1017. (d) Leibovitch, M.; Olovsson, G.; Sundarababu, G.; Ramamurthy, V.; Scheffer, J. R.; Trotter, J. *J. Am. Chem. Soc.* **1996**, *118*, 1219.

(5) (a) Baek, K.; Hwang, I.; Roy, I.; Shetty, D.; Kim, K. *Acc. Chem. Res.* **2015**, *48*, 2221. (b) Ni, X.-L.; Chen, S.; Yang, Y.; Tao, Z. *J. Am. Chem. Soc.* **2016**, *138*, 6177. (c) Kim, H. J.; Heo, J.; Jeon, W. S.; Lee, E.; Kim, J.; Sakamoto, S.; Yamaguchi, K.; Kim, K. *Angew. Chem. Int. Ed.* **2001**, *40*, 1526. (d) Maddipatla, M. V. S. N.; Kaanumalle, L. S.; Natarajan, A.; Pattabiraman, M.; Ramamurthy, V. *Langmuir* **2007**, *23*, 7545.

(6) (a) Yoshizawa, M.; Tamura, M.; Fujita, M. *Science* **2006**, *312*, 251. (b) Nishioka, Y.; Yamaguchi, T.; Kawano, M.; Fujita, M. *J. Am. Chem. Soc.* **2008**, *130*, 8160. (c) Alagesan, M.; Kanagaraj, K.; Wan, S.; Sun, H.; Su, D.; Zhong, Z.; Zhou, D.; Wu, W.; Gao, G.; Zhang, H. *J. Photochem. Photobiol., A* **2016**, 331, 95.

(7) (a) Bach, T.; Bergmann, H.; Grosch, B.; Harms, K. *Angew. Chem., Int. Ed.* **2000**, *39*, 2302. (b) Bauer, A.; Westkämper, F.; Grimme, S.; Bach, T. *Nature*, **2005**, *436*, 1139. (c) Brimioulle, R.; Bach, T. *Science* **2013**, *342*, 840.

(8) (a) Axel G. Griesbeck; Meierhenrich, U. J. *Angew. Chem. Int. Ed.* **2002**, *41*, 3147. (b) de Jong, J. J. D.; Lucas, L. N.; Kellogg, R. M.; van Esch, J. H.; Feringa, B. L. *Science* **2004**, *304*, 278. (c) Kuzmanich, G.; Vogelsberg, C. S.; Maverick, E. F.; Netto-Ferreira, J. C.; Scaiano, J.; Garcia-Garibay, M. A. *J. Am. Chem. Soc.* **2012**, *134*, 1115. (d) Lv, F.-F.; Chen, B.; Wu, L.-Z.; Zhang, L.-P.; Tung, C.-H. *Org. Lett.* **2008**, *10*, 3473. (f) Fan, C.; Wu, W.; Chruma, J. J.; Zhao, J.; Yang, C. *J. Am. Chem. Soc.* **2016**, 138, 15405. (g) Liang, W.; Zhao, Wei, X.; Yan, Z.; Wu, W.; Caldera, F.; Trotta, F.; Inoue, Y.; Su, D.; Zhong, Z.; Yang C. *RSC Adv.* **2017**, 7, 17184.

(9) (a) Hembury, G. A.; Borovkov, V. V.; Inoue, Y. *Chem. Rev.* .**2008**, *108*, 1 (b) Leung, D.; Kang, S. O.; Anslyn, E. V. *Chem.Soc. Rev*. **2012**, *41*, 448. (c) You, L.; Zha, D.; Anslyn, E. V. *Chem. Rev.* **2015**, *115*, 7840.

(10) (a) Becker, H. D. *Chem. Rev.* **1993**, *93*, 145. (b) Bouas-Laurent, H.; Desvergne, J.-P.; Castellan, A.; Lapouyade, R. *Chem. Soc. Rev.* **2000**, *29*, 43. (c) Bouas-Laurent, H.; Desvergne, J.-P.; Castellan, A.; Lapouyade, R. *Chem. Soc. Rev.* **2001**, *30*, 248.

(11) (a) Becker, H.-D.; Becker, H.-C.; Langer, V. *J. Photochem. Photobiol. A: Chem.* **1996**, *97*, 25. (b) Fages, F.; Desvergne, J.-P.; Frisch, I.; Bouas-Laurent, H. *Chem. Commun.* **1988**, 1413. (c) Horiguchi, M.; Ito, Y. *J. Org. Chem.* **2006**, *71*, 3608.

(12) (a) Tamaki, T. *Chem. Lett.* **1984**, 53. (b) Tamaki, T.; Kokubu, T.; Ichimura, K. *Tetrahedron Lett.* **1987**, *43*, 1485. (c) Tamaki, T.; Kokubu, T. *J. Incl. Phenom. Macrocycl. Chem* **1984**, *2*, 815.

(13) (a) Nakamura, A.; Inoue, Y. *J. Am. Chem. Soc.* **2003**, *125*, 966. (b) Yao, J.; Yan, Z.; Ji, J.; Wu, W.; Yang, C.; Nishijima, M.; Fukuhara, G.; Mori, T.; Inoue, Y. *J. Am. Chem. Soc.* **2014**, *136*, 6916. (c) Yang, C.; Ke, C.; Liang, W.; Fukuhara, G.; Mori, T.; Liu, Y.; Inoue, Y. *J. Am. Chem. Soc.* **2011**, *133*, 13786. (d) Ke, C.; Yang, C.; Mori, T.; Wada, T.; Liu, Y.; Inoue, Y. *Angew. Chem. Inter.Ed.* **2009**, *48*, 6675. (e) Yang, C.; Mori, T.; Origane, Y.; Ko, Y. H.; Selvapalam, N.; Kim, K.; Inoue, Y. *J. Am. Chem. Soc.* **2008**, *130*, 8574. (f) Yang, C.; Nakamura, A.; Wada, T.; Inoue, Y. *Org. Lett.* **2006**, *8*, 3005. (g) Yang, C.; Nakamura, A.; Fukuhara, G.; Origane, Y.; Mori, T.; Wada, T.; Inoue, Y. *J. Org Chem.* **2006**, *71*, 3126. (h) Yang, C.; Fukuhara, G.; Nakamura, A.; Origane, Y.; Fujita, K.; Yuan, D.-Q.; Mori, T.; Wada, T.; Inoue, Y. *J. Photochem. Photobiol. A: Chem.* **2005**, *173*, 375. (i) Nakamura, A.; Inoue, Y. *J. Am. Chem. Soc.* **2005**, *127*, 5338. (j) Kawanami, Y.; Katsumata, S.-y.; Nishijima, M.; Fukuhara, G.; Asano, K.; Suzuki, T.; Yang, C.; Nakamura, A.; Mori, T.; Inoue, Y. *J. Am. Chem. Soc.* **2016**, 138,12187.

(14) (a) Nishijima, M.; Wada, T.; Mori, T.; Pace, T. C. S.; Bohne, C.; Inoue, Y. *J. Am. Chem. Soc.* **2007**, *129*, 3478. (b) Fuentealba, D.; Kato, H.; Nishijima, M.; Fukuhara, G.; Mori, T.; Inoue, Y.; Bohne, C. *J. Am. Chem. Soc.* **2013**, *135*, 203.

(15) See the Supporting Information for details.

(16) (a) Hättig, C.; Weigend, F. *J. Chem. Phys*. **2000**, *113*, 5154. (b) Hättig, C.; Kohn, A. *J. Chem. Phys.* **2002**, *117*, 6939.

(17) Wakai, A.; Fukasawa, H.; Yang, C.; Mori, T.; Inoue, *Y. J. Am. Chem. Soc.* **2012**, *134*, 4990.

(18) (a) Grimme, S.; Antony, J.; Ehrlich, S.; Krieg, H. *J. Chem. Phys*. **2010**, *132*, 154104. (b) Grimme, S.; Ehrlich, S.; Goerigk, L. *J. Comput. Chem.* **2011**, *32*, 1456. (c) Tao, J.; Perdew, J. P.; Staroverov, V. N.; Scuseria, G. E. *Phys. Rev. Lett.* **2003**, *91*, 146401.

(19) Kajtár, M. H. T., C.; Kuthi, E.; Szejtli, J. *Acta. Chim. Acad. Sci. Hung.* **1982**, *110*, 327.

(20) (a) Hamai, S.; Hatamiya, A. *Bull. Chem. Soc. Jpn.* **1996**, *69*, 2469. (b) Barros, T. C.; Stefaniak, K.; Holzwarth, J. F.; Bohne C. *J. Phys. Chem. A* **1998**, *102*, 5639. (c) Tang, H.; Sutherland, A. S.; Osusky, L. M.; Li, Y.; Holzwarth, J. F.; Bohne, C. *Photochem. Photobiol. Sci.* **2014**, *13*, 358.

(21) Rekharsky, M. V.; Inoue, Y. *Chem. Rev.* **1998**, *98*, 1875.

(22) Fukuhara, G.; Iida, K.; Kawanami, Y.; Tanaka, H.; Mori, T.; Inoue, Y. *J. Am. Chem. Soc.* **2015**, *137*, 15007.

(23) Chandross, E. A.; Ferguson, J.; McRae, E. *J. Chem. Phys.* **1966**, *45*, 3546.

(24) (a) Yang, C.; Wang, Q.; Yamauchi, M.; Yao, J.; Zhou, D.; Nishijima, M.; Fukuhara, G.; Mori, T.; Liu, Y.; Inoue, Y. *Photochem. Photobiol. Sci.* **2014**, *13*, 190. (b) Wang, Q.; Yang, C.; Ke, C.; Fukuhara, G.; Mori, T.; Liu, Y.; Inoue, Y. *Chem. Commun.* **2011**, *47*, 6849.

(25) (a) Gonikberg, M. G.; Ewald, A. H. *J. Electrochem. Soc.* **1965**, *112*, 31C. (b) Van Eldik, R.; Asano, T.; LeNoble, W. *Chem. Rev.* **1989**, *89*, 549.

(26) Yang, C.; Mori, T.; Inoue, Y. *J. Org. Chem.* **2008**, *73*, 5786.

(27) Rohbach, R. P.; Rodriguez, L. J. R.; Eyring, E. M. *J. Phys. Chem.* **1977**, *81*, 944.

(28) Marcus, Y. *Ion Solvation*; Wiley: New York, 1985, p. 107.

(29) (a) McGlynn, S. P.; Sunseri, R.; Christodoules, N. *J. Chem. Phys.* **1962**, *37*, 1818. (b) Patterson, L. K.; Rzad, S. J. *Chem. Phys. Lett*. **1975**, *31*, 254. (c) Homer, R. B.; Allsopp, S. R. *Biochim. Biophys. Acta* **1976**, *434*, 297. (d) Radaram, B.; Mako, T.; Levine, M. *Dalton Trans*. **2013**, 42, 16276.

(30) Murov, S. L.; Carmichael, I.; Hug, G. L. *Handbook of Photochemistry*, 2nd ed.; Marcel Dekker: New York, 1993.

(31) Reichardt, C.; Welton, T. *Solvents and Solvent Effects in Organic Chemistry*, 4th ed.; Wiley-VCH: Weinheim, 2010.

(32) (a) Wentworth Jr, P.; Janda, K. D. *Cell Biochem. Biophys.* **2001**, *35*, 63. (b) Keinan, E. *Catalytic Antibodies*; Wiley-VCH: Weinheim, 2005.

TOC

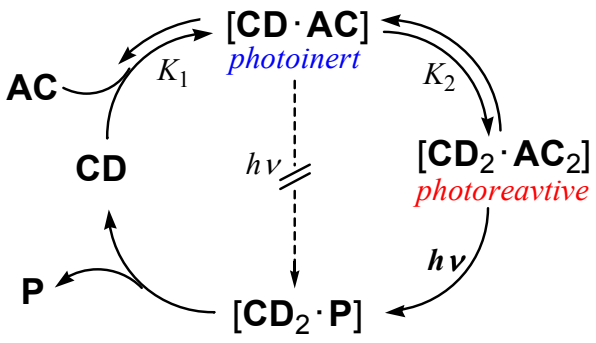
[CD · AC]
photoinert
AC
K_1
K_2
CD
$h\nu$
[CD$_2$ · AC$_2$]
photoreavtive
$h\nu$
P
[CD$_2$ · P]